ORNL/TM-8449

ornl

OAK
RIDGE
NATIONAL
LABORATORY

UNION
CARBIDE

Analysis of the Creep Strain-Time Behavior of Alloy 800

M. K. Booker

METALS and CERAMICS
ENERGY
RESEARCH
DEVELOPMENT
OAK RIDGE NATIONAL LABORATORY

OPERATED BY
UNION CARBIDE CORPORATION
FOR THE UNITED STATES
DEPARTMENT OF ENERGY

Printed in the United States of America. Available from
National Technical Information Service
U.S. Department of Commerce
5285 Port Royal Road, Springfield, Virginia 22161
NTIS price codes—Printed Copy: A04; Microfiche A01

ORNL/TM-8449

METALS AND CERAMICS DIVISION

ANALYSIS OF THE CREEP STRAIN-TIME BEHAVIOR OF ALLOY 800

M. K. Booker

Date Published - May 1983

Prepared by the
OAK RIDGE NATIONAL LABORATORY
Oak Ridge, Tennessee 37830
operated by
UNION CARBIDE CORPORATION
for the
U.S. Department of Energy
under Contract No. W-7405-eng-26

CONTENTS

ANALYSIS OF THE CREEP STRAIN-TIME BEHAVIOR OF ALLOY 800*

M. K. Booker

ABSTRACT

The high-nickel austenitic alloy 800 (in both the mill-annealed and the solution-treated grades) has several attractive properties that make it a good candidate for service at elevated temperatures in corrosive environments. One such property is creep resistance. This report analyzes the elevated-temperature creep behavior of the mill-annealed grade, generally referred to simply as alloy 800. (The solution-treated grade is known as alloy 800H.) Available data over the temperature range from 538 to 760°C were collected and evaluated to yield mathematical approximations for creep-rupture and creep strain-time behavior for use in design calculations. However, the creep behavior of this material is extremely complex, and the analysis presented here contains substantial uncertainties. All results in this report should be considered preliminary because of limited data currently available.

INTRODUCTION

The high-nickel austenitic alloy 800 (in both the mill-annealed and the solution-treated grades) has several attractive properties that make it a good candidate for service at elevated temperatures in corrosive environments.[1] One such property is creep resistance. We have analyzed the elevated-temperature creep behavior of the mill-annealed grade, generally referred to simply as alloy 800. (The solution-treated grade is known as alloy 800H.) Available data were collected and evaluated to yield mathematical approximations for creep-rupture and creep strain-time behavior for use in design calculations. All results given in this report are analytically valid from 450 to 760°C and at stresses from zero to the ultimate tensile strength at temperature. However, extrapolation beyond

*Research performed for Sandia National Laboratories on Integrated Contractor Purchase Order No. 92-9105 with funding supplied by the U.S. Department of Energy.

the actual range of data should be done with caution. Moreover, the creep behavior of this material is extremely complex, and the analysis presented here contains substantial uncertainties. All results in this report should be considered preliminary.

DATA

Available creep data consisted of information obtained from Huntington Alloys[2] and from the Tampa Division of Westinghouse Electric Company.[3] The total creep-rupture data base consisted of 116 tests on 16 lots* of material conducted over the temperature range from 450 to 760°C, with rupture lives extending from 10 h to about 19,000 h. Measurements of the 0.2% offset time-to-tertiary creep (91 tests) and minimum creep rate (94 tests) were available for most of these tests. However, actual strain-time creep curves were available for only 43 tests, all from Huntington Alloys. Within the time frame of this investigation, the creep curves from the Westinghouse tests (~34 tests) could not be located. This small number of creep curves dictates that any conclusions drawn concerning the creep strain-time behavior of this material be considered preliminary and interim. Table 1 summarizes the characteristics of the lots of material for which data were available, and Table 2 summarizes the available data.

CREEP-RUPTURE BEHAVIOR

The available creep-rupture data were analyzed with the generalized regression treatment of lot-centered data, as described elsewhere.[4] Essentially, this method allows one to examine a large number of mathematical models for materials behavior and to choose the one that best represents the available data. Moreover, the use of lot-centered data allows one to treat data from many lots of material simultaneously while still retaining the individual strength characteristics of each lot. The appendix describes the lot-centered regression approach in more detail.

---

*A "lot" of material is defined as material expected to have the same properties because of common composition and processing history. Often a lot is one heat or one product form of a heat.

Table 1. Chemical composition of heats of alloy 800

Heat	Content[a] (%)									
	C	N	Cu	Ti	Ni	Mn	Cr	Si	Al	S
HH5501A	0.07	0.014	0.54	0.44	33.71	0.91	20.54	0.45	0.38	0.007
HH6729A	0.02	0.009	0.26	0.54	34.13	0.79	20.30	0.50	0.27	0.003
HH7094A	0.03	0.02	0.63	0.41	32.94	0.76	20.85	0.36	0.38	0.002
HH9315A	0.04		0.37		31.79	0.92	20.69	0.35		0.007
L00111XT	0.031			0.41	31.40	0.76	20.10	0.22	0.31	0.003
Plate										
HH3283A										
HH8808A	0.05		0.26	0.56	31.16	0.79	21.53	0.39	0.52	0.007
Round bar										
HH8735A	0.04		0.38	0.43	31.31	0.50	21.24	0.40	0.28	0.007
Sched 80 pipe										
HH8311A	0.09		0.69	0.40	32.95	0.78	22.19	0.34	0.42	0.007
Tube										
570594	0.024	0.02		0.34	33.40		21.20	0.49	0.27	
FY0531/1	0.02	0.015	0.04	0.42	33.60	0.56	19.40	0.38	0.20	0.006
FY0531/6/1	0.02	0.015	0.04	0.42	33.60	0.56	19.40	0.38	0.20	0.006
HH1929A	0.04	0.013	0.27	0.42	31.63	0.80	19.80	0.36	0.41	0.007
HH2658A	0.08		0.41	0.31	31.18	1.04	21.39	0.57	0.20	0.007
HH5341A	0.03		0.34	0.37	30.73	0.89	20.83	0.34	0.46	0.007
HH5464A	0.06	0.013	0.57	0.45	32.81	0.83	20.24	0.40	0.44	0.007
HH5959A	0.04		0.46	0.50	32.18	0.83	19.82	0.31	0.43	0.007
HH6225A	0.04		0.51	0.53	32.28	0.86	21.89	0.44	0.50	0.007
HH7382A	0.07		0.62	0.52	32.30	0.77	20.50	0.32	0.52	0.007
HH7391A	0.07		0.44	0.53	32.26	0.82	20.80	0.32	0.52	0.007

[a]Balance iron.

Table 2. Alloy 800 creep data

Heat	Temperature (°C)	Stress (MPa)	Minimum creep rate (%/h)	Time to tertiary creep (h)	Total elongation (%)	Rupture life (h)
570594	500	308.9		1,990	4.76	2,622
570594	500	308.9		6,010	8.33	11,141
570594	500	316.6		6,980	5.95	8,110
570594	500	324.3		4,360	5.95	5,512
570594	500	346.0		1,540	7.10	2,192
570594	500	374.5			13.70	697
570594	600	108.1		7,400	7.24	11,543
570594	600	123.6		4,500	7.74	8,006
570594	600	139.0		3,900	7.10	6,360
570594	600	216.2		83	17.30	128
570594	600	231.7			17.90	70
FY0531/1	450	463.3			31.80	6,745
FY0531/1	500	324.3		12,000	13.60	17,842
FY0531/1	500	366.0			17.10	3,779
FY0531/1	500	373.8		1,770	17.00	1,773
FY0531/1	500	383.0			20.40	1,117
FY0531/1	600	139.0			6.81	9,937
FY0531/1	600	216.2			9.10	1,027
FY0531/1	600	231.7			20.40	148
FY0531/6/1	500	308.9		18,500	11.90	18,742
FY0531/6/1	600	231.7		2,500	7.74	2,520
HH1929A	538	206.9	3.00 E-05			
HH1929A	538	241.3	1.20 E-04			
HH1929A	593	172.4	1.90 E-04			
HH1929A	593	310.3			50	27
HH1929A	649	55.2	9.00 E-05	2,880		
HH1929A	649	82.7	5.40 E-04	900		
HH1929A	649	137.9			28	350
HH1929A	649	206.9			50	30
HH2658A	538	379.2			30	41
HH2658A	593	275.8			42	42
HH2658A	649	172.4			30	61
HH3283A	550	273.7				5,400
HH3283A	550	293.7			28	2,054
HH3283A	550	293.7			26	3,932
HH3283A	550	313.7			38	1,500
HH3283A	550	313.7			36	1,754
HH3283A	550	342.7			41	410
HH3283A	550	342.7			41	615
HH3283A	550	372.3			39	99
HH3283A	550	392.3			51	47

Table 2. (Continued)

Heat	Temperature (°C)	Stress (MPa)	Minimum creep rate (%/h)	Time to tertiary creep (h)	Total elongation (%)	Rupture life (h)
HH3283A	600	206.2			16	5,334
HH3283A	600	224.8			29	974
HH3283A	600	224.8			17	2,897
HH3283A	600	244.8			25	216
HH3283A	600	244.8			16	1,091
HH3283A	600	293.7			55	39
HH5341A	538	379.2			30.50	103
HH5341A	593	103.4	3.00 E–05			
HH5341A	593	275.8			38.50	69
HH5341A	649	172.4			30.50	97
HH5464A	538	275.8	2.80 E–04	1,410		
HH5464A	538	327.5	7.50 E–03	740	60	1,447
HH5464A	538	344.8	1.53 E–03	518	181	972
HH5464A	538	365.4	6.82 E–02	216		
HH5501A	538	344.8	2.10 E–02	430	45.20	742
HH5501A	593	241.3	3.40 E–03	400	23.30	989
HH5959A	538	206.9	5.00 E–05			
HH5959A	538	379.2			27	200
HH5959A	593	103.4				
HH5959A	593	275.8	3.30 E–04	235	13	736
HH5959A	649	68.9	3.00 E–05			
HH5959A	649	147.5	9.00 E–04	380	20	873
HH6225A	593	172.4	3.70 E–04	728		
HH6729A	538	344.8	8.30 E–03	700	39	1,372
HH6729A	593	206.9	1.40 E–04	7,267	10.80	13,187
HH6729A	593	241.3	1.70 E–04	1,410	9	4,726
HH6729A	593	296.5	2.40 E–02	168	33	361
HH7094A	538	234.4	2.00 E–05	17,231		
HH7094A	538	258.6	8.00 E–04	6,367		16,861
HH7094A	538	344.8	2.20 E–02	385	41	678
HH7094A	593	172.4	5.20 E–04	2,485	37	7,006
HH7094A	593	241.3	8.60 E–03	390	28.20	753
HH7382A	593	172.4	1.10 E–04	635		
HH7391A	593	172.4	2.50 E–04	880		
HH8311A	593	172.4	5.00 E–05			
HH8735A	538	241.3		3,099		
HH8735A	538	275.8	4.00 E–05			
HH8735A	538	344.8	1.80 E–04	1,155	21	21
HH8735A	538	413.7	5.10 E–02	54	46.50	121
HH8735A	593	172.4	6.00 E–05			

Table 2. (Continued)

Heat	Temperature (°C)	Stress (MPa)	Minimum creep rate (%/h)	Time to tertiary creep (h)	Total elongation (%)	Rupture life (h)
HH8735A	593	206.9	6.00 E-05			
HH8735A	593	241.3	1.43 E-03	316		
HH8735A	593	275.8	2.90 E-02	171	31.50	271
HH8735A	593	344.8	0.52	9		16
HH8735A	621	124.1	7.00 E-05	4,610		
HH8735A	649	82.7	6.00 E-05			
HH8735A	649	103.4	3.10 E-04	3,120	21.50	8,034
HH8735A	649	137.9	2.27 E-03	530	45	1,440
HH8735A	649	206.9	0.11	49	51	111
HH8735A	649	241.3	0.80	10	61.50	20
HH8735A	704	31.0	1.20 E-04			
HH8735A	760	27.6	1.20 E-04			
HH8735A	760	41.4	3.27 E-03	1,490	36.50	3,554
HH8735A	760	68.9	0.11	171	58.50	241
HH8735A	760	82.7	0.44	41	84	78
HH8808A	482	482.7	8.70 E-03	407	51	807
HH8808A	538	173.8				
HH8808A	538	344.8	3.10 E-03	1,520	18	1,942
HH8808A	538	379.2	7.23 E-03	380	21.50	728
HH8808A	538	413.7	7.50 E-02	100	40	178
HH8808A	593	206.9	1.90 E-04	3,370	6	4,886
HH8808A	593	241.3	1.00 E-04	2,450	5	4,722
HH8808A	593	275.8	1.10 E-03	965	10	1,373
HH8808A	593	344.8	0.75	26	39.50	32
HH8808A	593	344.8	0.79	33	45	39
HH8808A	621	96.5	5.00 E-05	1,900		
HH8808A	621	96.5	5.00 E-05			
HH8808A	621	137.9	8.00 E-05	2,750	5	6,259
HH8808A	621	172.4	2.70 E-04	1,210	13.50	2,807
HH8808A	621	275.8	6.40 E-02	93	18.50	110
HH8808A	649	55.2				
HH8808A	649	68.9	4.00 E-05	2,920		
HH8808A	649	137.9	1.45 E-03	405	19.60	1,359
HH8808A	649	149.4	3.30 E-03	415	15	870
HH8808A	649	172.4	5.28 E-03	162	15.50	440
HH8808A	649	206.9	1.41 E-02	157	17.50	300
HH8808A	649	275.8	3.90	5	64	6
HH8808A	704	31.0	1.00 E-04			
HH8808A	704	41.4	4.00 E-04	1,250	33	8,081
HH8808A	704	82.7	1.00 E-04	100	50	802

Table 2. (Continued)

Heat	Temperature (°C)	Stress (MPa)	Minimum creep rate (%/h)	Time to tertiary creep (h)	Total elongation (%)	Rupture life (h)
HH8808A	704	137.9	0.18	27	71	64
HH8808A	704	206.9	11.0	2	76.50	3
HH8808A	760	13.8				
HH8808A	760	17.2				
HH8808A	760	20.7	1.40 E–04	3,170		
HH8808A	760	27.6	8.00 E–04	790	54.50	4,611
HH8808A	760	41.4	9.80 E–03	645	46.50	1,484
HH8808A	760	68.9	9.46 E–02	18	74	146
HH8808A	760	89.6	0.49	15	76.50	42
HH9315A	510	344.8	4.20 E–04	2,856	27.20	5,548
HH9315A	538	324.1	6.50 E–04	1,000	27.50	1,819
HH9315A	538	324.1	8.90 E–04	950	28.80	2,236
HH9315A	538	356.5	3.30 E–02	197	40.50	316
HH9315A	538	356.5	2.00 E–02	318	37.50	516
HH9315A	538	356.5	1.20 E–02	415	35	637
HH9315A	538	375.8	7.50 E–02	100	45.70	149
HH9315A	538	375.8	5.50 E–02	136	43	201
HH9315A	538	388.9	8.70 E–02	26	49.30	108
HH9315A	593	226.8	8.70 E–03	685	22.50	1,002
HH9315A	593	226.8	5.50 E–03	700	15.60	1,090
HH9315A	593	239.9	1.10 E–02	525	22.70	736
HH9315A	649	142.7	4.60 E–03	284	36	726
HH9315A	649	142.7	4.20 E–03	400	36	917
HH9315A	649	142.7	3.60 E–03	380	39.50	928
HH9315A	649	142.7	3.00 E–03	390	35.30	1,759
HH9315A	649	162.0	2.00 E–02	186	40	415
HH9315A	649	194.4	0.18	36	48.50	83
L00111XT	500	339.8			25	5,597
L00111XT	500	386.1			34	1,575
L00111XT	600	200.8			10	4,682
L00111XT	600	231.7			17	1,419

The equation selected to describe the creep rupture data for this material was

$$\log t_r = C_h - 2.557 \log \sigma + 22{,}090/T - 9.216\sigma/T \ , \qquad (1)$$

where

t_r = rupture life (h),
σ = stress (MPa),
T = temperature (K).

All logarithms used in this report are base 10. The parameter C_h is the "lot constant." It is used to reflect variations in strength among different lots. Average behavior is reflected by inserting an average value for the lot constant in the above equation. For these data, the average value of C_h is −14.067. The coefficient of determination (R^2) for the fit is 82.8%. The variance due to uncertainties within a lot (V_w) is 0.0805, and the variance due to uncertainties between lots (V_B) is 0.115. The overall variance (V) is the sum of these two, and the overall standard error of estimate (SEE = $\sqrt{V}$) is 0.442. An approximate lower limit on the strength of a given lot can be estimated by using the lot constant for that lot minus $1.65\sqrt{V_w}$, while an appropriate lower bound on the strength of the material can be estimated by using the average lot constant minus 1.65 SEE. Table 3 lists lot constants for the individual lots.

Figure 1 illustrates predictions obtained from the above equation in comparison with data for individual lots. (In this figure the solid lines indicate the predicted mean behavior for the lots shown and the dashed lines represent mean minus 1.65 within-lot standard errors in log time.) Figure 2 compares the predicted average behavior for the mill-annealed material from Eq. (1) with estimated average behavior for solution-annealed alloy 800H obtained[5] from lot-centered regression analysis. As can be seen, the long-term creep-rupture strength of alloy 800 is reasonably comparable to that of alloy 800H, although there is some indication that at higher temperatures and longer times the H grade exhibits a strength advantage.

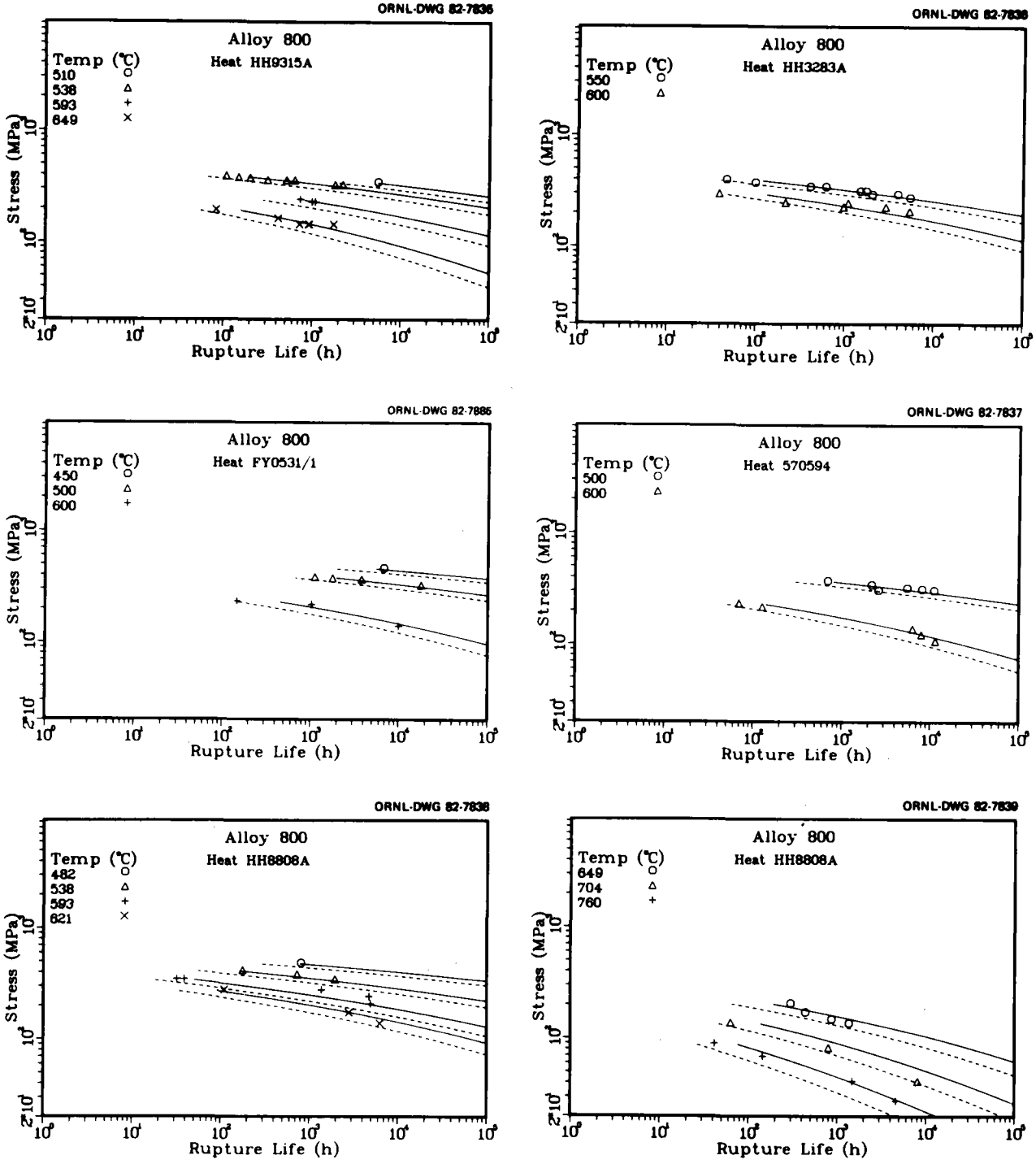

Fig. 1. Comparison of predicted and experimental creep-rupture behavior of five lots of alloy 800. Solid lines are predicted average behavior; dashed lines are predicted minimum behavior for each lot.

Table 3. Lot constants for alloy 800 creep data

Lot	Stress-rupture data		Minimum creep rate data	
	Number of data	Lot constant	Number of data	Lot constant
LC0111XT	4	−13.94		
570594	11	−14.73		
FY0531/1	8	−14.23		
FY0531/6/1	2	−13.83		
HH8808A	23	−13.75	28	22.74
HH5959A	3	−13.83	4	22.69
HH5341A	3	−14.45	1	24.06
HH2658A	3	−14.72		
HH8735A	11	−14.01	19	22.78
HH5464A	2	−13.89	4	23.37
HH1929A	3	−14.49	5	23.68
HH6225A			1	23.49
HH7382A			1	22.97
HH7391A			1	23.32
HH8311A			1	22.62
HH3283A	15	−13.85		
HH9315A	18	−14.03	18	23.37
HH6729A	4	−13.40	4	22.53
HH7094A	4	−14.00	5	23.60
HH5501A	2	−13.91	2	23.38

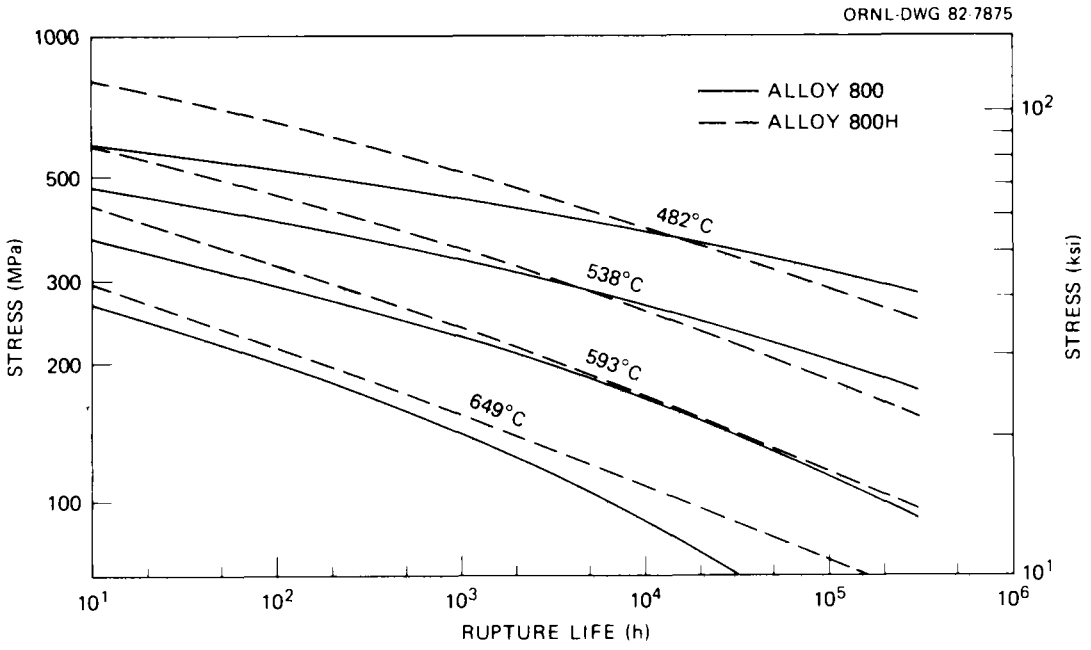

Fig. 2. Comparison of the predicted average creep-rupture behavior of mill-annealed alloy 800 and solution-annealed alloy 800H.

MINIMUM CREEP RATE

The available minimum creep rate data were analyzed by methods analogous to those used to examine the creep rupture data. The equation used to describe these data is

$$\log \dot{e}_m = C_h + 2.492 \log \sigma - 30{,}520/T + 13.8\sigma/T \ , \qquad (2)$$

where $\dot{e}_m$ is the minimum creep rate (%/h). The average lot constant for this equation is 23.137, and the value of R^2 is 81.3%. The between-lot variance is 0.105, and the within-lot variance is 0.291. The overall SEE is 0.629. Figure 3 compares predictions from Eq. (2) with minimum creep rate data for individual lots. These plots show a noticeably greater data scatter relative to the creep-rupture data, reflecting the complexity in the creep strain-time behavior of this material, as described below. Table 3 lists the individual lot constants for the 14 lots for which minimum creep rate data were available.

TIME TO TERTIARY CREEP

For purposes of this investigation, the onset of tertiary creep was defined by a 0.2% strain offset from linear secondary creep, as shown schematically in Fig. 4. When analyzed directly, the data for time to tertiary creep were well described by

$$\log t_{ss} = C_h - 1.966 \log \sigma + 18220/T - 7.02\sigma/T \ , \qquad (3)$$

where t_{ss} is the time to tertiary creep (h). The average lot constant for this equation is −11.874, and the value of R^2 is 81.3%. The between-lot variance is 0.0857, and the within-lot variance is 0.0938. The overall SEE is 0.424.

Another common method for analysis of time to tertiary creep data involves expression of t_{ss} as a function of the rupture life.[6-8] For these data, this relationship was found to be (Fig. 5)

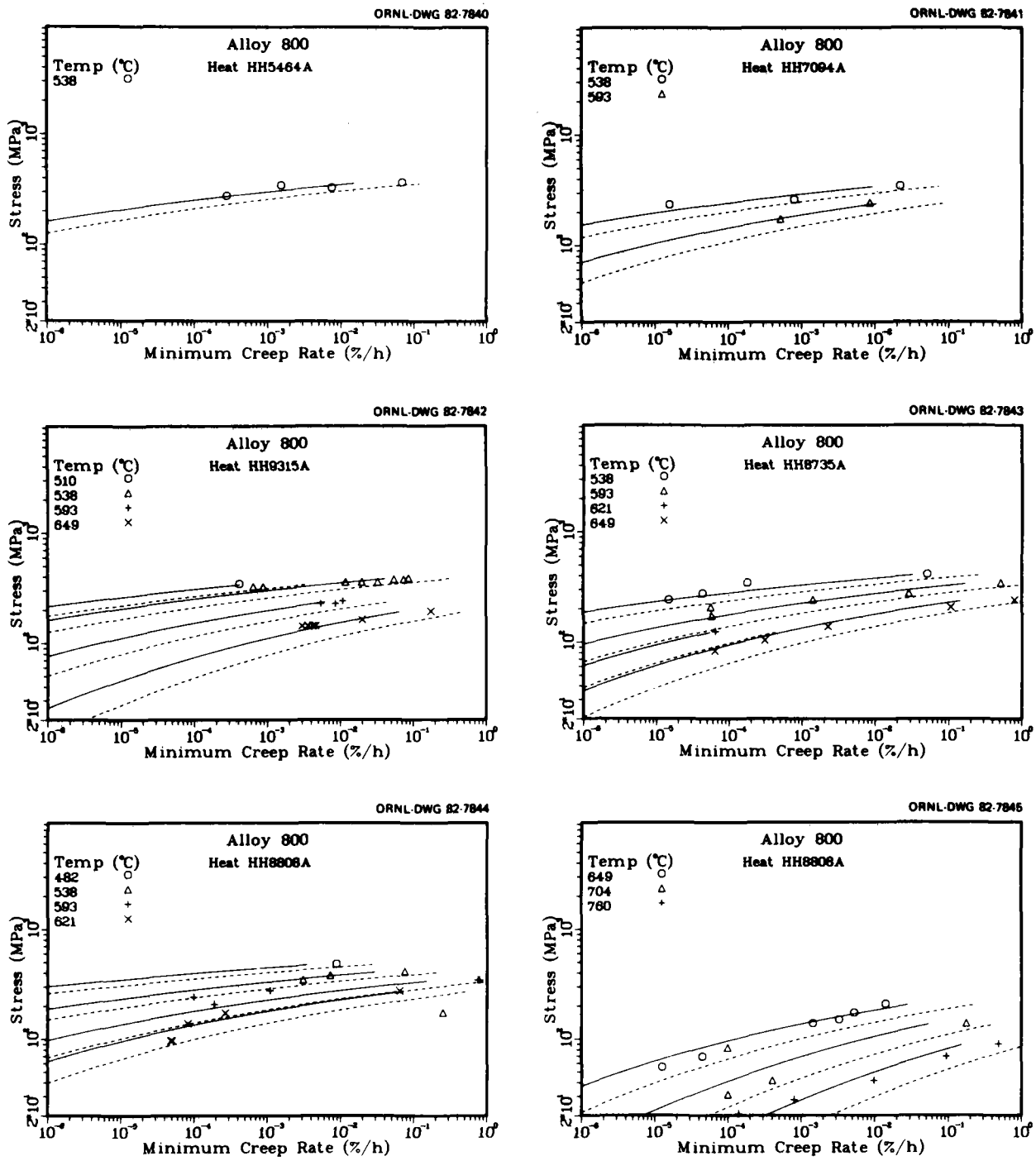

Fig. 3. Comparison of predicted and experimental minimum creep rate values of five lots of alloy 800. Solid lines are predicted average behavior, dashed lines predicted minimum behavior for each lot.

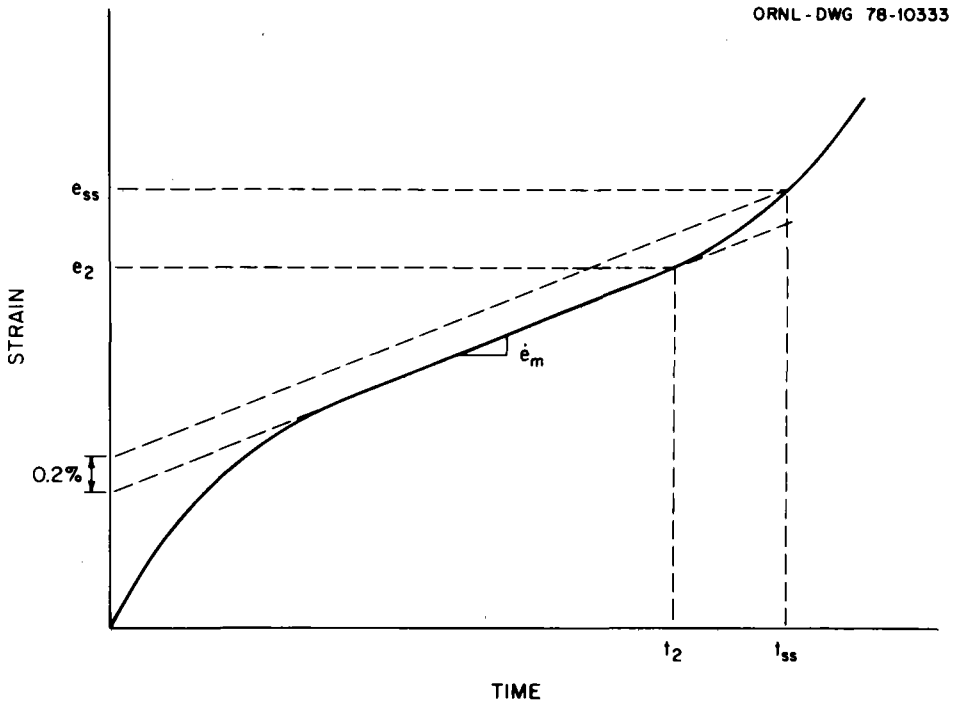

Fig. 4. Schematic definition of the onset of tertiary creep. The 0.2% offset time is labeled t_{ss}.

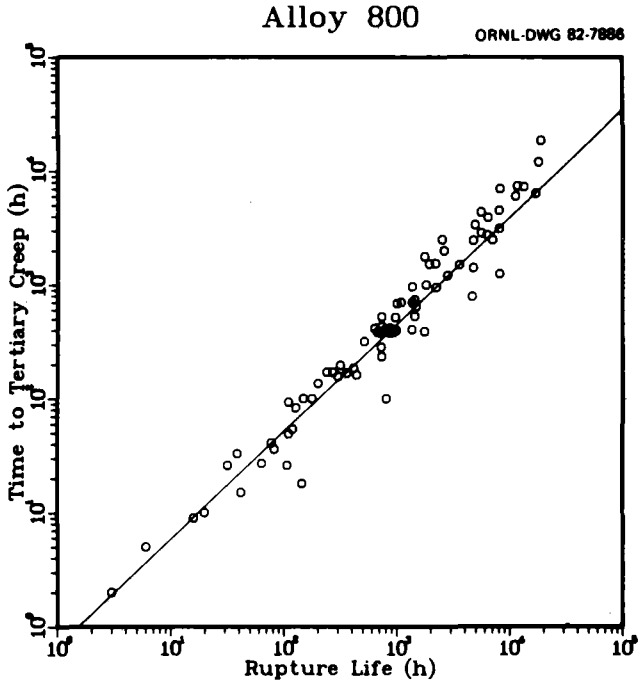

Fig. 5. Relationship between time to tertiary creep and rupture life for alloy 800.

$$t_{ss} = 0.67 t_r^{0.942} \quad . \tag{4}$$

A similar relationship was found earlier[8] for the 800H grade, although there the relationship appeared temperature dependent for temperatures above 866 K (593°C)

$T \leq 866$ K $\qquad t_{ss} = 0.726 t_r^{0.996}$ (5)

$T > 866$ K $\qquad t_{ss} = 0.000628^{6108/T} t_r^{0.996}$. (6)

The data for the current investigation showed no clear temperature dependence, although they spanned a smaller range of high temperature than did the 800H data (450–760°C vs 538–871°C).

Figure 6 compares available data for time to the onset of tertiary creep with predictions obtained by both the above methods. In general, the two sets of predictions are quite similar. We recommend use of Eq. (4) for design calculations, because that equation guarantees analytical consistency with the predictions for rupture behavior.

CREEP STRAIN-TIME BEHAVIOR

Analysis of creep strain-time data was complicated both by the storage of available data and by the fact that alloy 800 appears to display several types of creep curves. A recent survey[9] of 250 creep curves on both alloy 800 and alloy 800H identified ten generic creep curve shapes, as shown schematically in Fig. 7. After preliminary analysis, we determined that it would not be desirable to include alloy 800H in our investigation, because its behavior can be decidedly different from that of the mill-annealed alloy 800. Even so, most of the curve shapes shown in Fig. 7 were represented even within our small set of data. Figure 8, taken from Harrod, Langford, and Moon,[9] summarizes available creep curves for the mill-annealed form of heat HH8808A, which formed the largest part of our data base. According to those authors, all ten curve shapes were

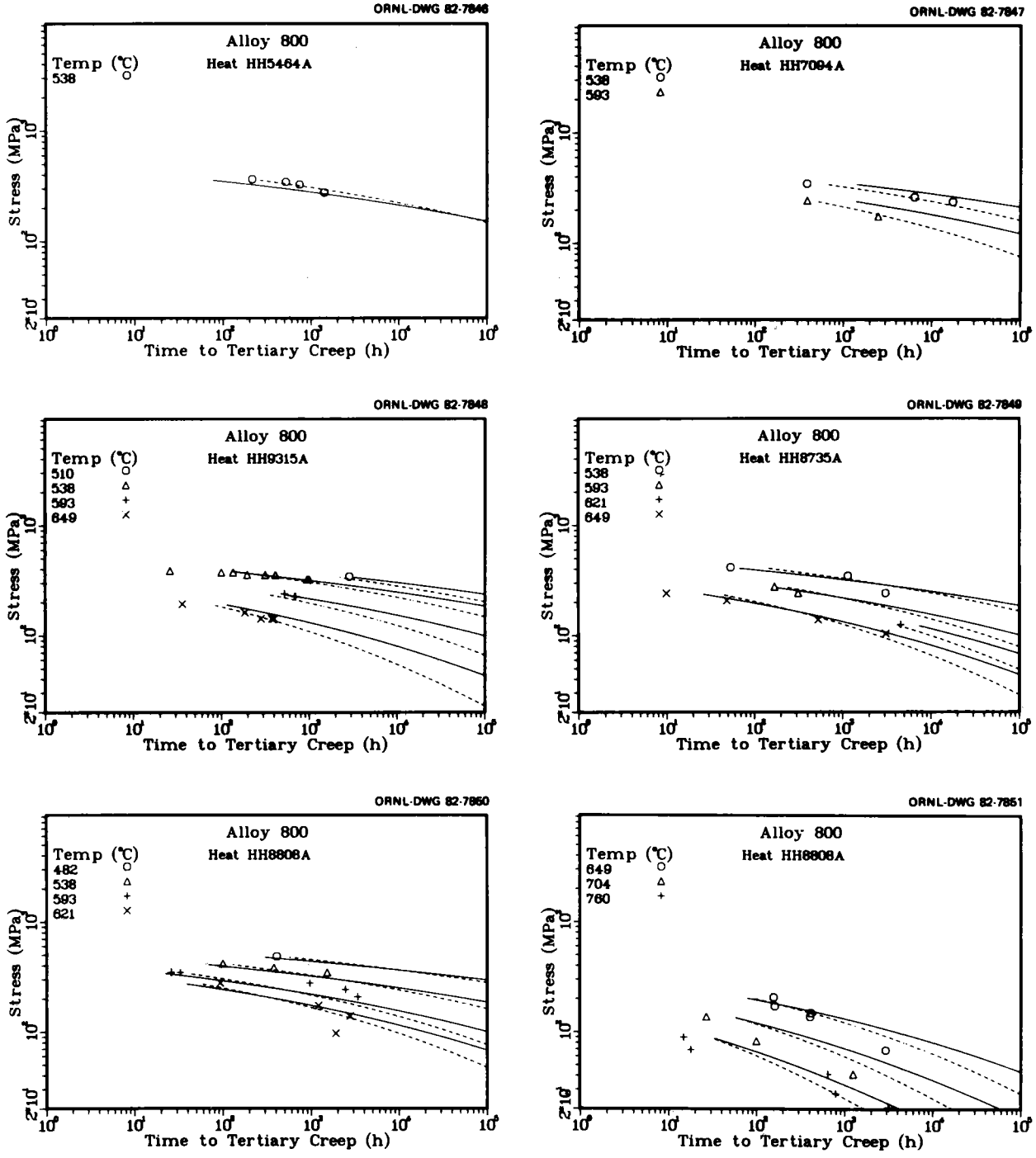

Fig. 6. Comparison of predicted and experimental values of time to tertiary creep for five lots of alloy 800. Solid lines are predicted from relationship with rupture life, dashed lines from direct fits to tertiary creep data.

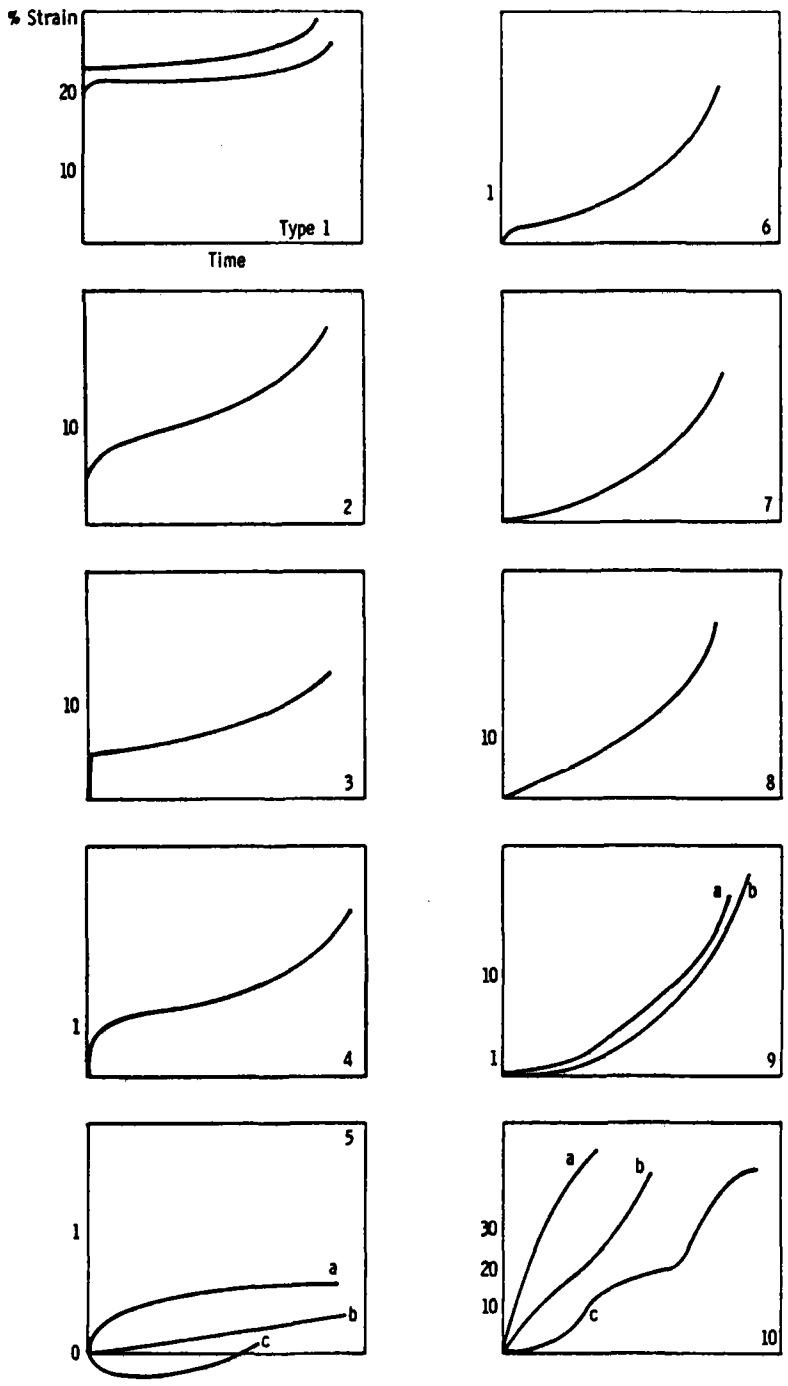

Fig. 7. Schematic illustration of the various creep curve shapes observed in alloy 800 and alloy 800H. Taken from D. L. Harrod, P. J. Langford, and D. M. Moon, "Relation of Physical Metallurgy to Mechanical Creep Behavior of Alloy 800," pp. 195–269 in *Status of Incoloy Alloy 800 Development for Breeder Reactor Steam Generators*, ORNL/SUB-4308/3, December 1978.

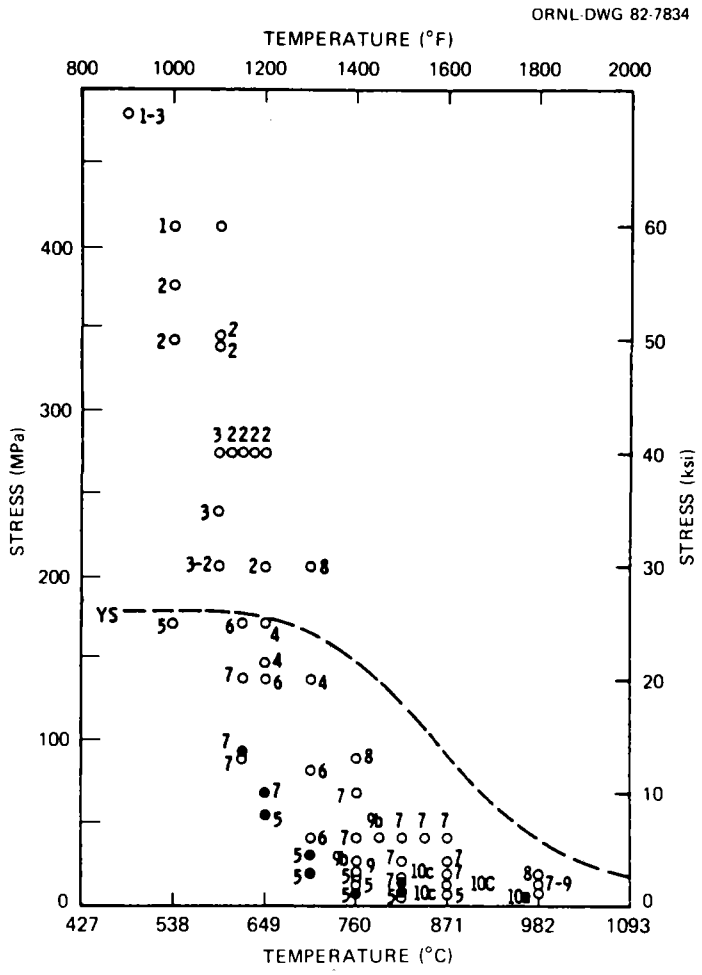

Fig. 8. Summary of creep tests for heat HH8808A of alloy 800. Numbers indicate creep curve type from Fig. 7. Source of data: D. L. Harrod, P. J. Langford, and D. M. Moon, "Relation of Physical Metallurgy to Mechanical Creep Behavior of Alloy 800," pp. 195–269 in *Status of Incoloy Alloy 800 Development for Breeder Reactor Steam Generators*, ORNL/SUB-4308/3, December 1978.

observed for this heat. In general, there is a trend for the higher numbered curve shapes to correspond to higher temperatures. (Note that within the temperature range of this investigation, only curve types 1 through 8 were observed.)

Clearly, the classical "creep equation" method often used for design with high-temperature materials[10-12] cannot be used here. (This approach generally assumes one generic curve shape, with parameters that vary with stress and temperature.) Therefore, to simplify analysis we reduced the individual creep curves to specify measured points corresponding to 0.1,

Table 4. Creep data of alloy 800 in terms of times to selected strains

Heat	Temperature (°C)	Stress (MPa)	Time (h) to strains of						Rupture time (h)
			0.1%	0.2%	0.5%	1%	2%	5%	
HH6729A	538	234	3,400	10,000					
HH6729A	538	258		3,500					
HH6729A	538	345				40	70	430	1,372
HH8735A	538	241		30	140				
HH8735A	538	276		24	160	2,340			
HH8735A	538	345		4	9	40	1,200	2,000	2,114
HH8735A	538	414		2	7	18	35	80	120
HH8735A	593	138		25					
HH8735A	593	172			30	1,000			
HH8735A	593	207			3	20	1,560		
HH8735A	593	276				2	20	88	271
HH8735A	621	124			75	1,980			
HH8735A	649	83	40	400					
HH8735A	649	103	11	36	770	1,450	2,270	4,240	8,034
HH8735A	649	138			3	12	25	740	1,440
HH8735A	649	207				1	3	25	111
HH8735A	704	31	10,450						
HH8808A	482	483	9	22	65	125	230	480	807
HH8808A	538	345			6	20	90	1,070	1,942
HH8808A	538	379			4	15	40	380	728
HH8808A	538	414		2	4	9	20	56	178
HH8808A	593	207			280	2,640	3,940		4,886
HH8808A	593	241		3	700	3,040	4,470		4,722
HH8808A	593	276			2	5	400		1,373
HH8808A	593	345					2	5	32
HH8808A	593	345						3	39
HH8808A	607	276					2	160	337
HH8808A	621	96.5	1,530	2,400					
HH8808A	621	96.5	1,900	2,760					
HH8808A	621	138	1,100	1,720	2,900	4,050	5,170		6,258
HH8808A	621	172	77	480	1,050	1,560	2,150		2,807
HH8808A	621	276					1	10	110
HH8808A	649	55	1,800						
HH8808A	649	69	1,460	2,400	3,750	5,440			
HH8808A	649	138		7	100	350	600	950	1,359
HH8808A	649	149			6	50	310	620	870
HH8808A	649	172		5	30	83	195	335	440
HH8808A	649	207				1	5	160	300
HH8808A	704	21							
HH8808A	704	31	1,320	1,890					
HH8808A	704	41	150	370	880	1,400	2,180	3,820	8,081
HH8808A	704	83		18	64	135	202	338	802
HH8808A	704	138				1	4	19	64

Our first approach was to attempt a pointwise analysis of the data in Table 4, giving separate equations for the times to each strain level similar to that for rupture life above. Creep curves could then be constructed by interpolating between the different strain levels.[13-14] Unfortunately, we had to abandon this approach because of lack of data at many strain levels and corresponding lack of consistency among the predicted times at different strain levels.

The approach we finally used is similar to that used by Sterling[15] for the alloy 800H material. Essentially, he used the above pointwise approach but constrained the results at different strains to be related by a simple power law:

$$e_c = Ct^n \ , \tag{7}$$

where

e_c is the creep strain (%),

t is the time (h),

C, n are functions of stress and temperature.

Sterling further specified that stress and temperature dependence be represented by a Larson-Miller parameter.

We used the above approach with two modifications. First we used an equation form for stress and temperature dependence identical to that used above for t_r, $\dot{e}_m$, and t_{ss} rather than a Larson-Miller parameter. Second, we analyzed data for $e_c \leq 1\%$ and for $e_c \geq 1\%$ separately, obtaining two different power laws and greater flexibility for data description.

The results of this analysis are summarized in the following equations:

$e_c \geq 1\%$

$$\log t = C_h - 2.475 \log \sigma + 36{,}000/T - 15.650\sigma/T + 0.324 \log e_c$$

$$+ 1020.4(\log e_c)/T \ , \tag{8}$$

$e_c \leq 1\%$

$$\log t = C_h - 3.792 \log \sigma + 27{,}190/T - 9.383\sigma/T - 0.492 \log e_c + 1292.6(\log e_c)/T \ . \quad (9)$$

The fits of these equations can be summarized as follows:

Eq.	Number of Data	R^2 (%)	V_B	V_W	SEE (log t)
(8)	77	81.3	0.263	0.248	0.715
(9)	87	68.9	0.588	0.411	1.000

The very large values of the standard error of estimate in log time are indicative of the extreme uncertainties involved in predicting behavior with this method. This uncertainty is due largely to variations in material behavior itself.

The resulting prediction of strain-time behavior is illustrated schematically in Fig. 9. Note that Eqs. (8) and (9) were not constrained to match exactly at 1% strain. Therefore, the interface between the two

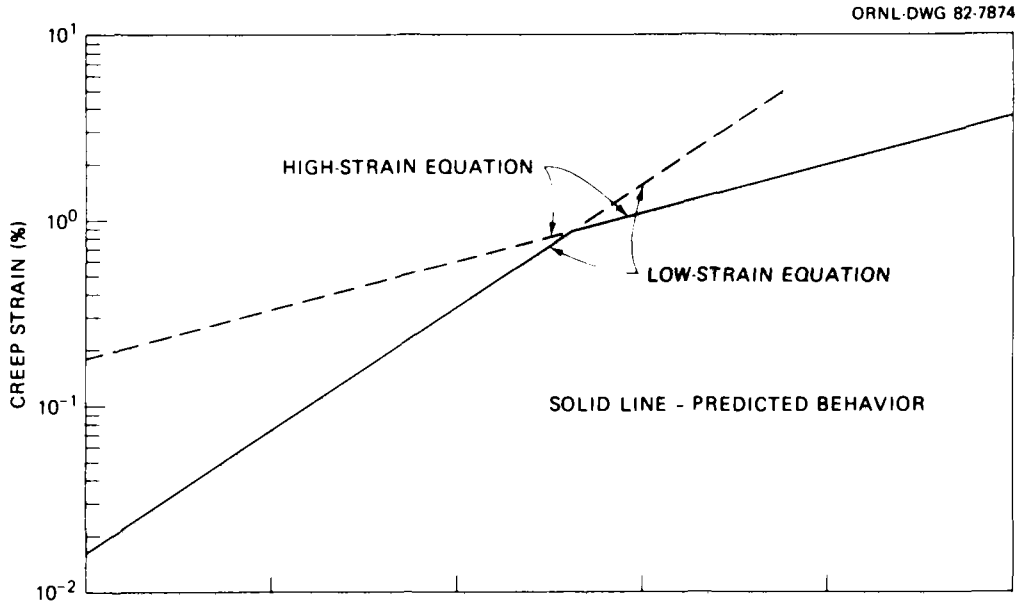

Fig. 9. Schematic illustration of the bilinear power law creep equation.

equations will not occur exactly at 1% strain but wherever the equations happen to match. Since (over the range of applicability of these equations) Eq. (9) always predicts a smaller partial derivative of log t with respect to log e_c, the relevant equation in any circumstance is the one that predicts the larger time value for a given strain value.

Figures 10 through 12 compare predictions of the above equations with actual strain-time data values from Table 4. Again, note the large amount of uncertainty in these predictions. However, we feel that the current predictions are the best that can be obtained from the data available for examination in this investigation. Figures 13 through 18 compare experimental data and predictions for specific strain values.

Since only three lots of material were factored into the fits of Eqs. (8) and (9), we could not obtain a reasonable estimate of the overall average lot constants for this material directly from the data. Various normalization schemes based on the relative positions of these three heats in the analysis of rupture data were tried, but none were found satisfactory. However, heat HH8735A was found to be very nearly an average strength heat in the rupture analysis. Therefore, we suggest that average strain-time behavior be predicted by using the lot constants for heat HH8735A. In our judgment, it is not possible to derive a meaningful estimate of the strain-time behavior of a lot of minimum strength from these data. The lot constants for the three available lots are summarized in Table 5.

Table 5. Lot constants for creep strain-time behavior of alloy 800

Lot	Equation (8)		Equation (9)	
	Number of data	Lot constant	Number of data	Lot constant
HH8735A	23	−29.610	29	−18.521
HH6729A	3	−29.956	4	−17.415
HH8808A	51	−29.180	54	−17.780

Note that the above creep strain-time predictions are only valid for times less than t_{ss}, as described above.

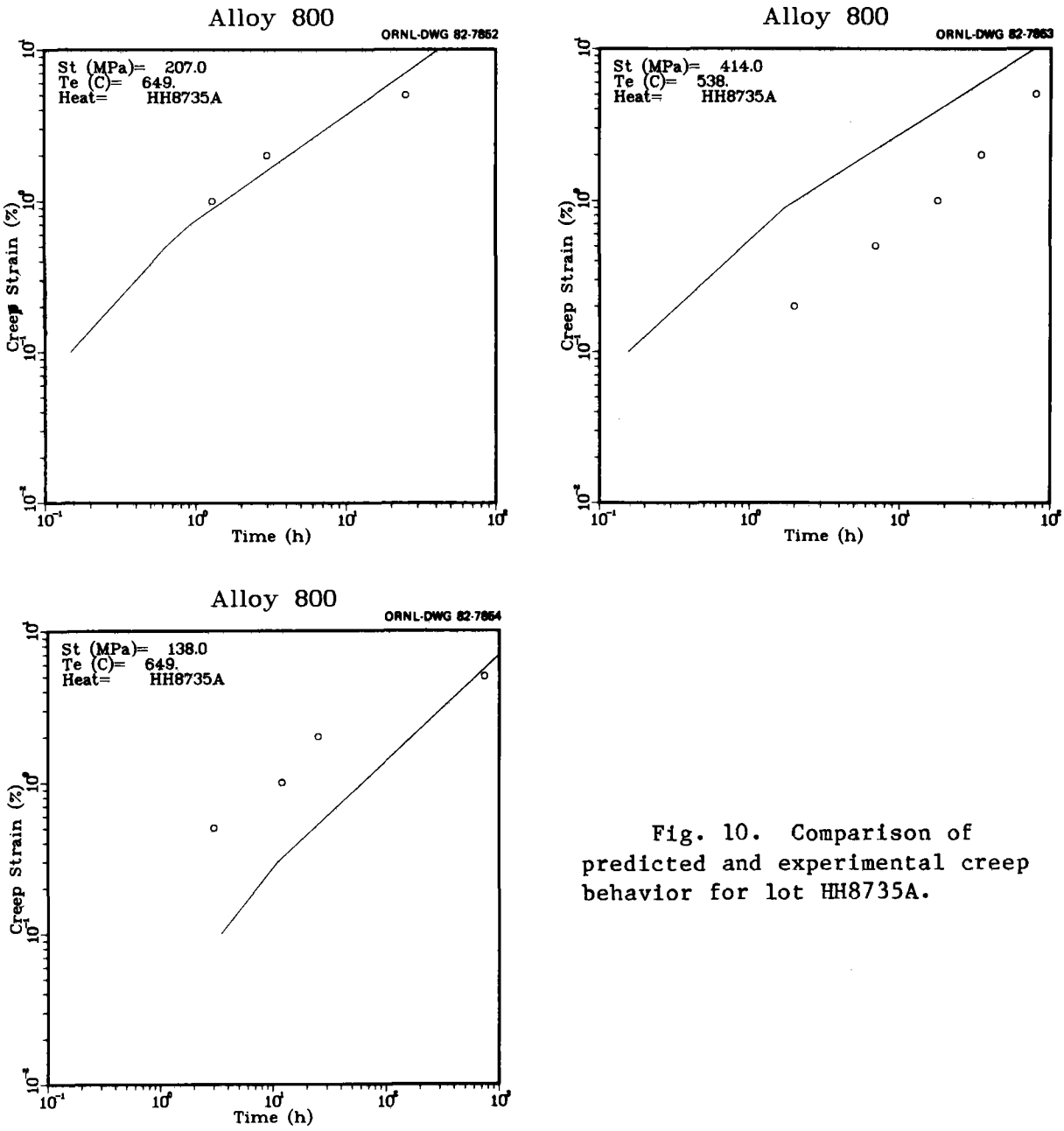

Fig. 10. Comparison of predicted and experimental creep behavior for lot HH8735A.

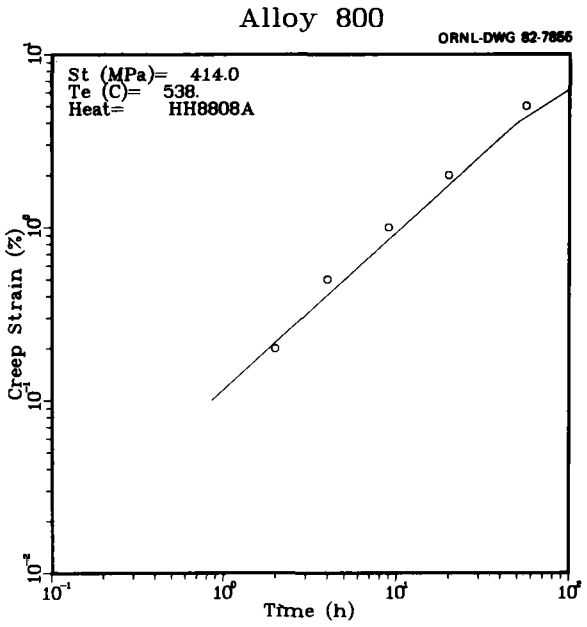

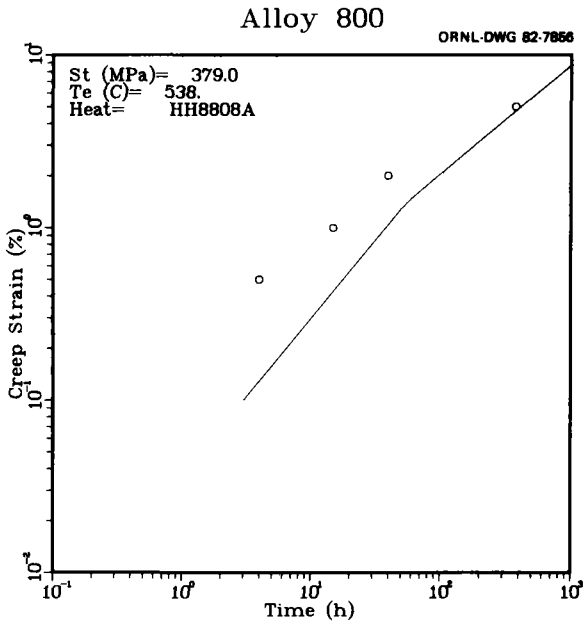

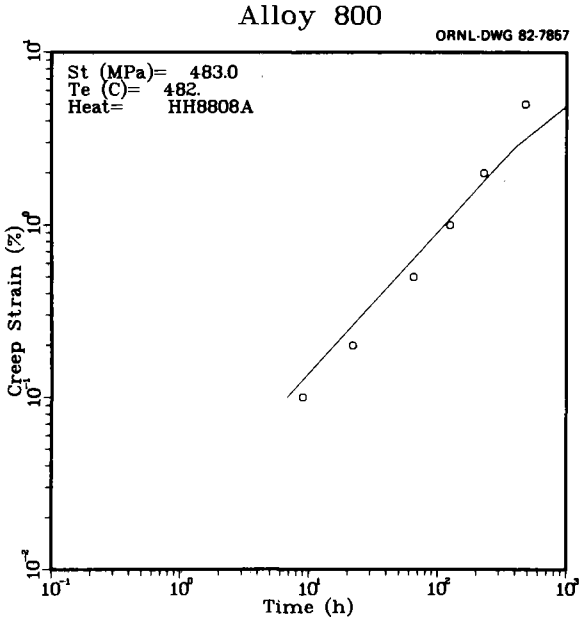

Fig. 11. Comparison of predicted and experimental creep behavior for lot HH8808A at 482 and 538°C.

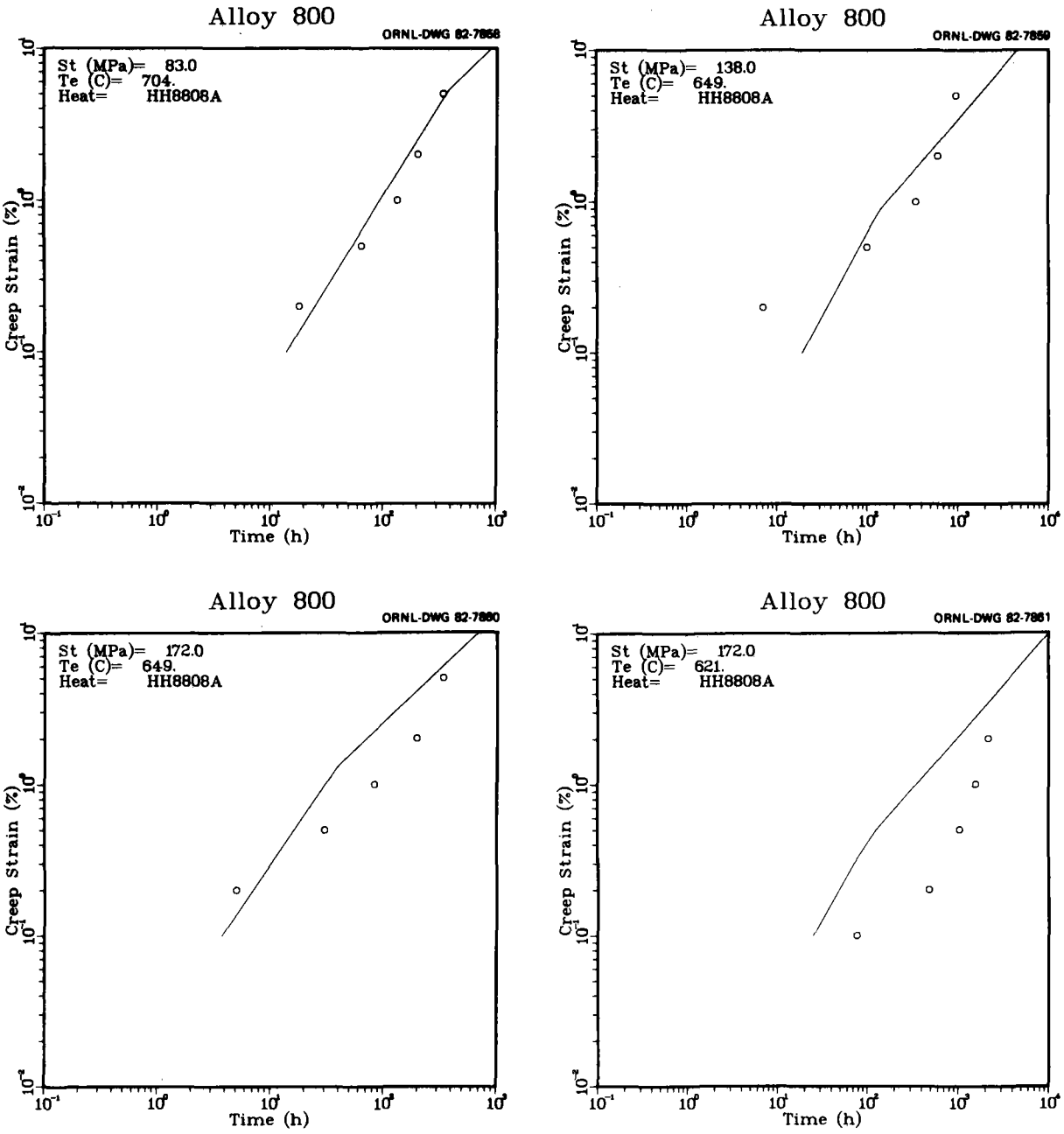

Fig. 12. Comparison of predicted and experimental creep behavior for lot HH8808A at 621, 649, and 704°C.

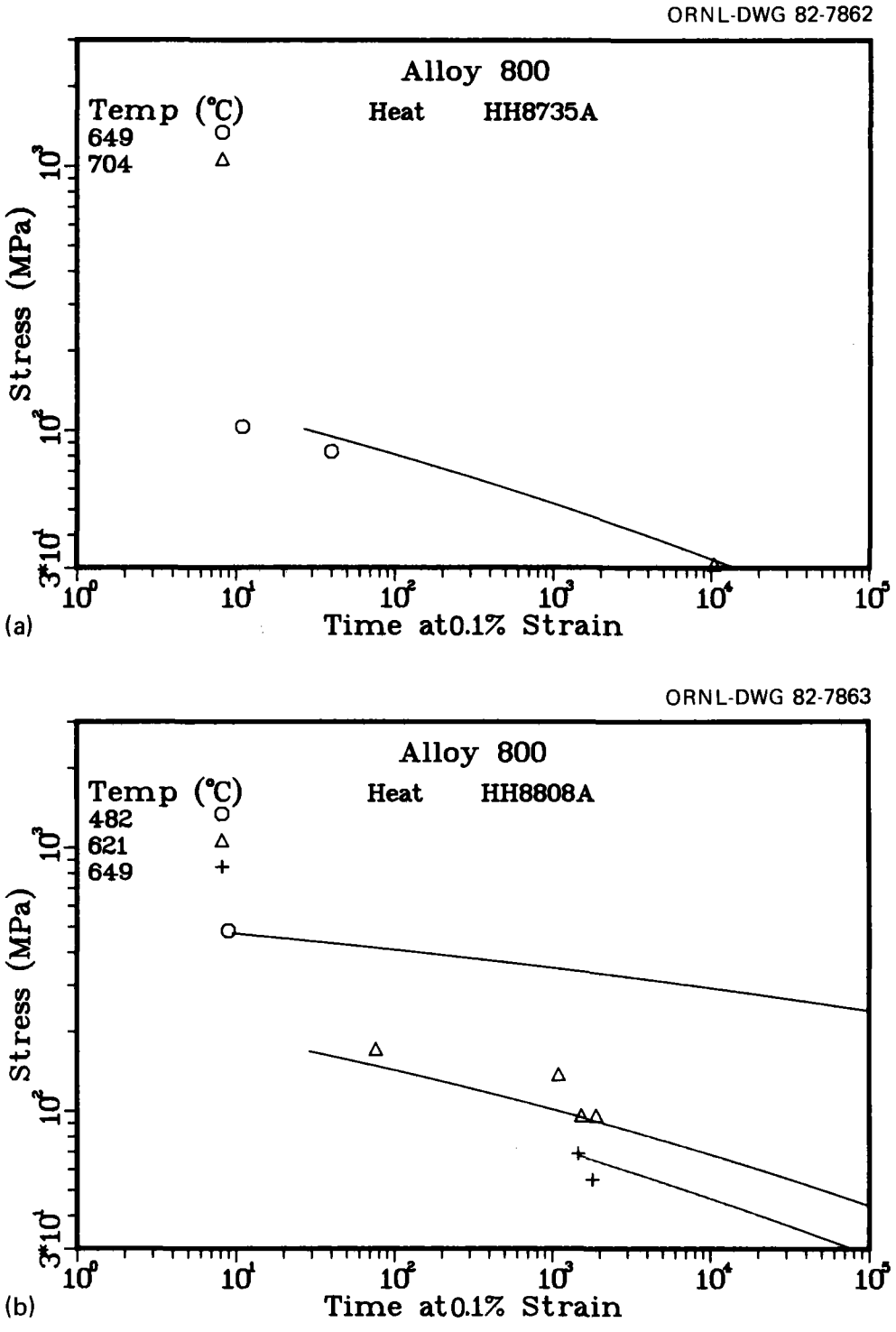

Fig. 13. Comparison of predicted and experimental values of time to 0.1% creep strain for (a) heat HH8735A and (b) heat HH8808A of alloy 800.

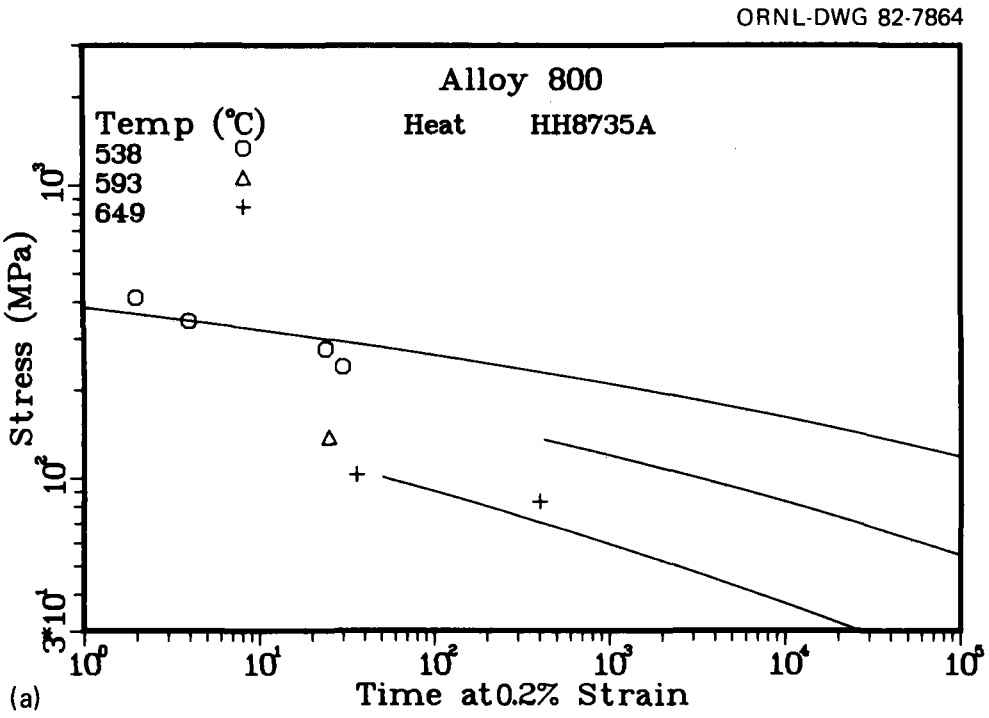

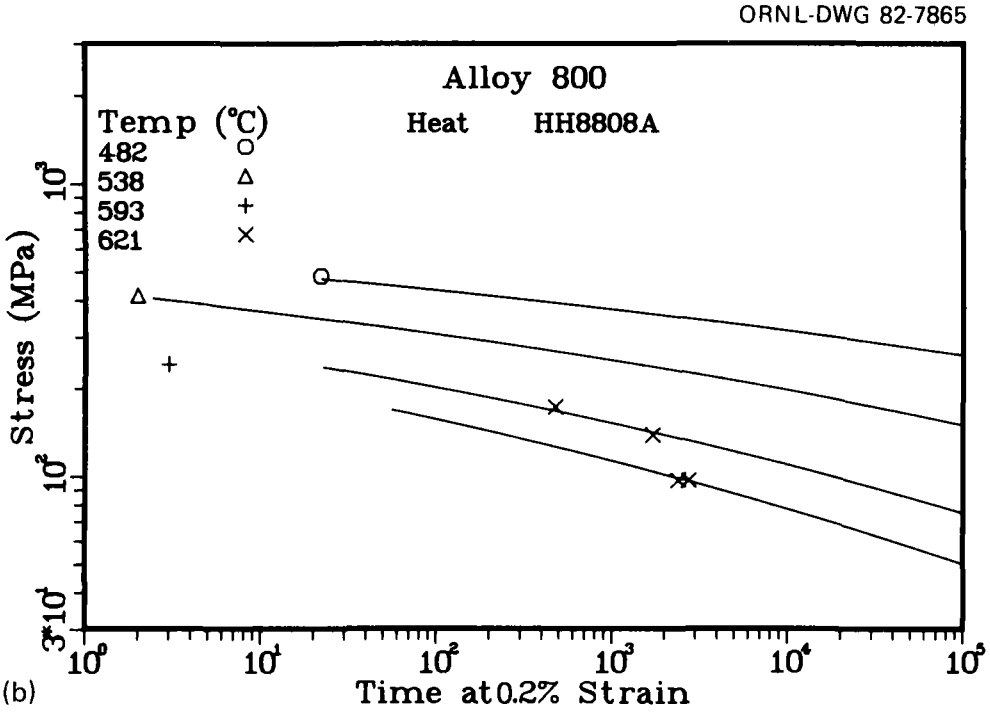

Fig. 14. Comparison of predicted and experimental values of time to 0.2% creep strain for (a) heat HH8735A and (b) heat HH8808A of alloy 800.

ORNL-DWG 82-7866

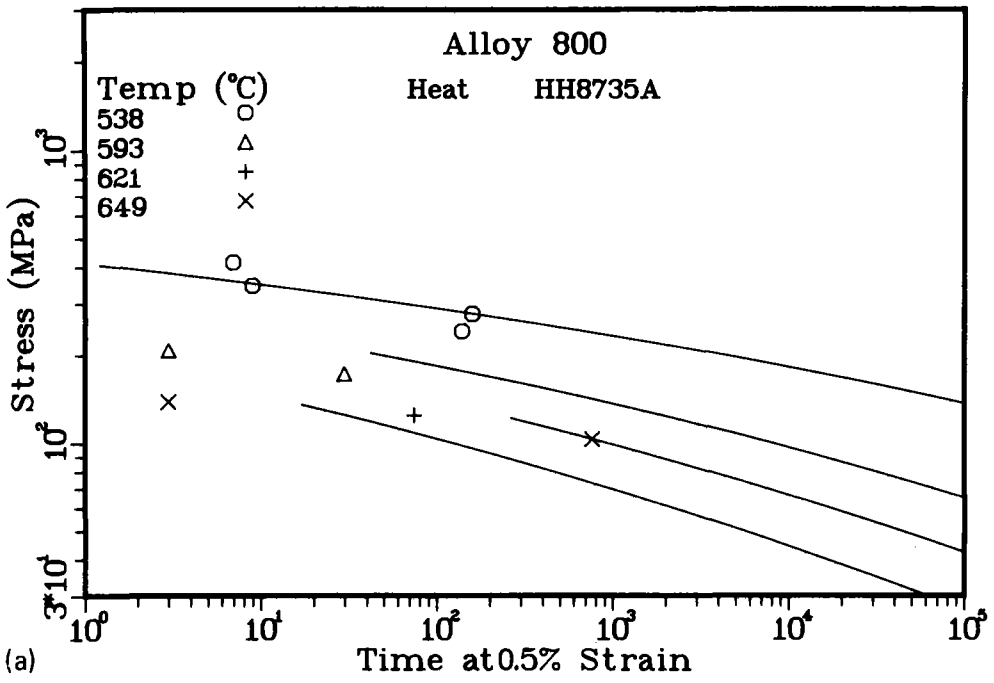

(a)

ORNL-DWG 82-7867

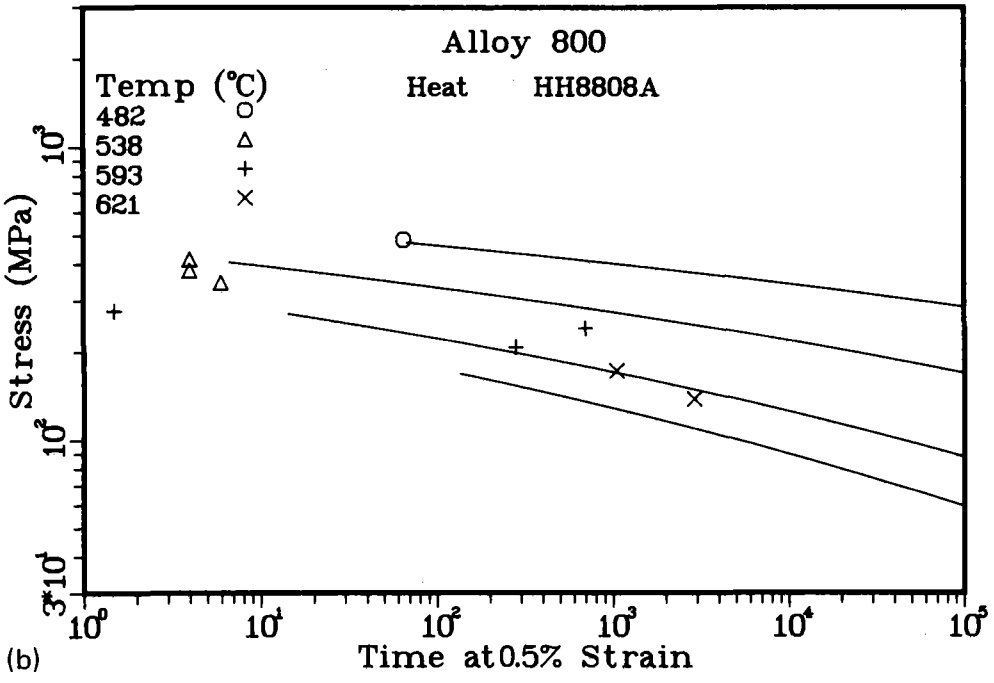

(b)

Fig. 15. Comparison of predicted and experimental values of time to 0.5% creep strain for (a) heat HH8735A and (b) heat HH8808A of alloy 800.

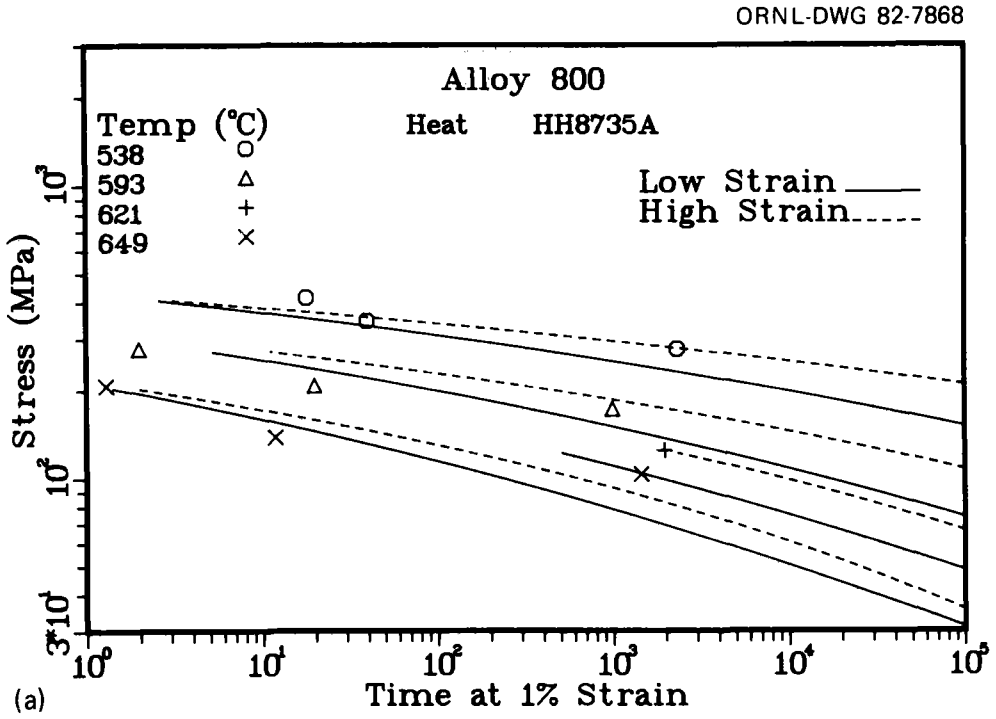

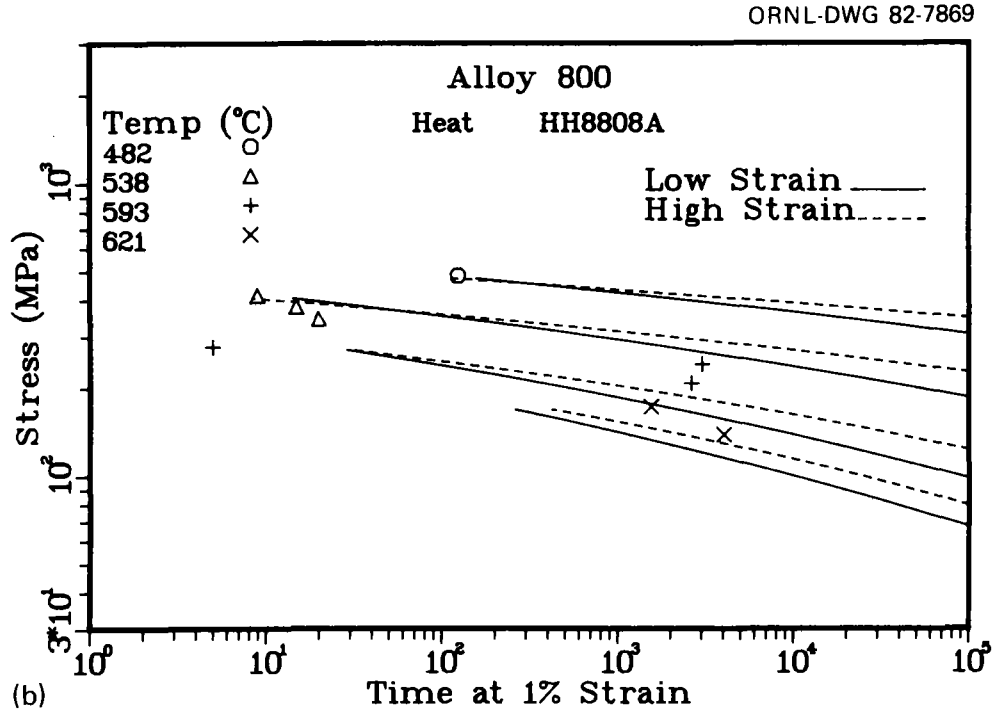

Fig. 16. Comparison of predicted and experimental values of time to 1.0% creep strain for (a) heat HH8735A and (b) heat HH8808A of alloy 800.

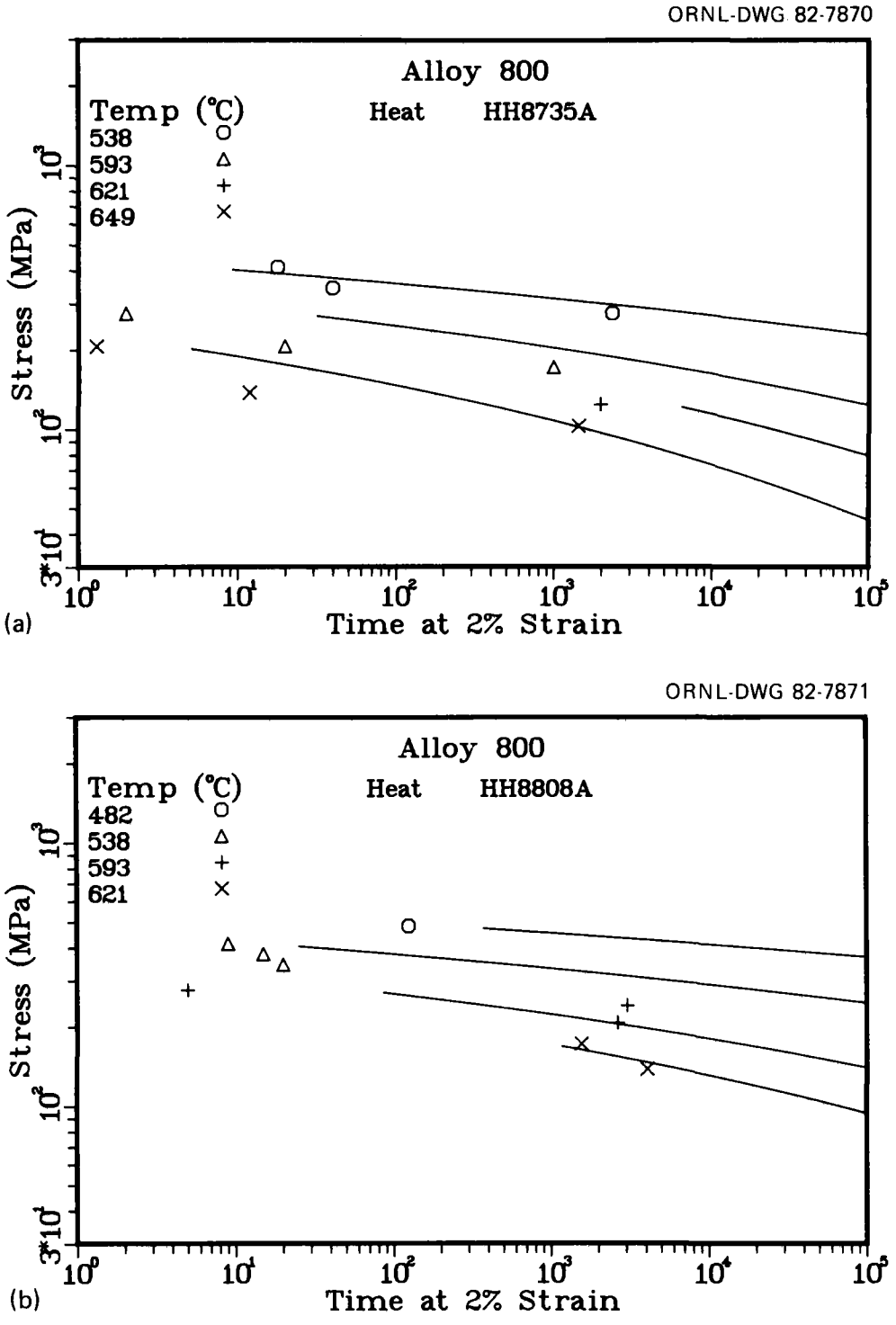

Fig. 17. Comparison of predicted and experimental values of time to 2.0% creep strain for (a) heat HH8735A and (b) heat HH8808A of alloy 800.

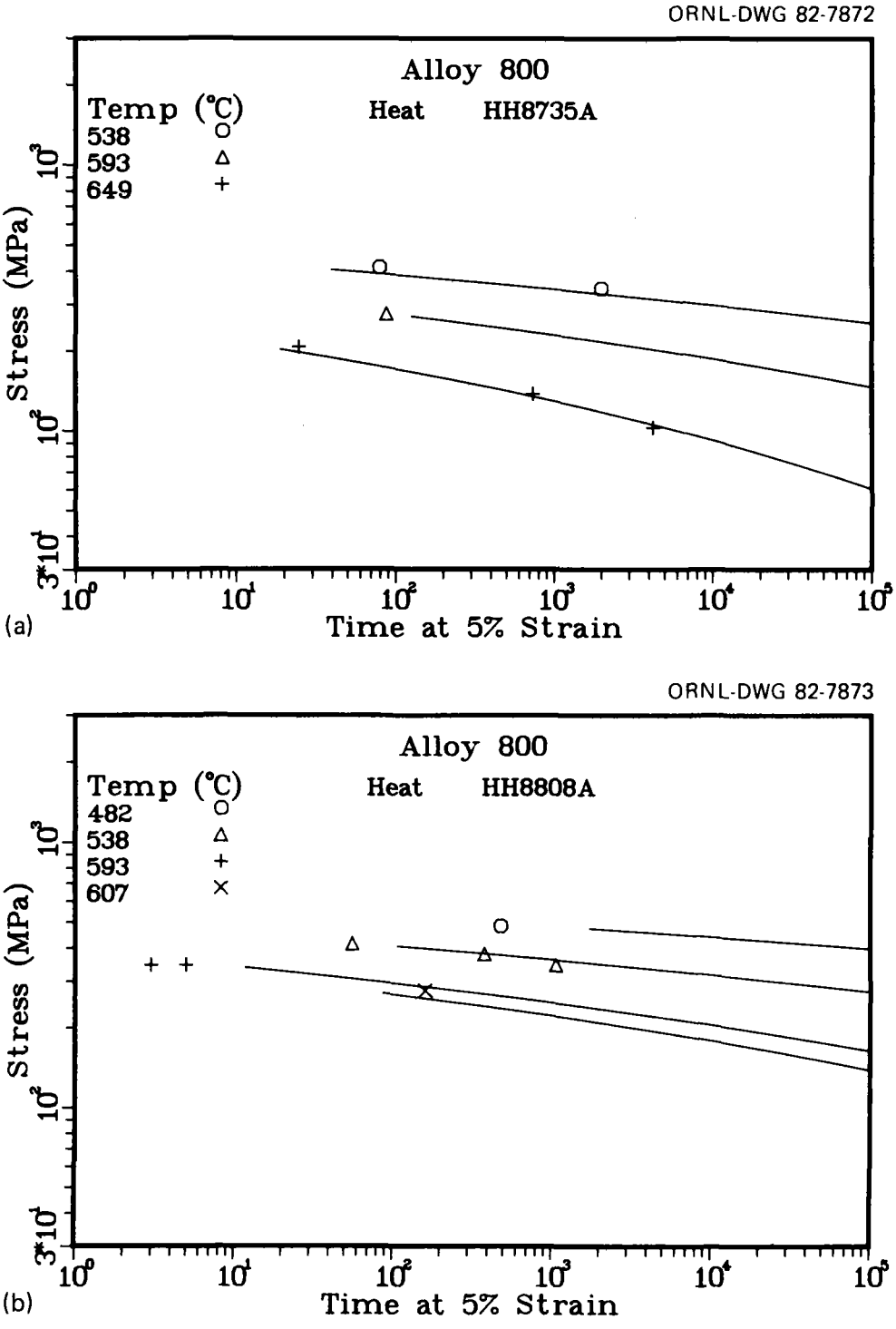

Fig. 18. Comparison of predicted and experimental values of time to 5.0% creep strain for (a) heat HH8735A and (b) heat HH8808A of alloy 800.

Figures 19 and 20 compare average isochronous stress-strain curves obtained from the above creep strain-time analysis with those derived previously[16] for alloy 800H. (Tensile stress-strain behavior was assumed to be the same for both material grades, so any differences in these figures are due strictly to differences in predicted creep strain-time behavior.) The trends shown in these figures are consistent with those seen earlier for rupture life. At longer times and higher temperatures the mill-annealed material becomes significantly weaker than the solution-annealed material.

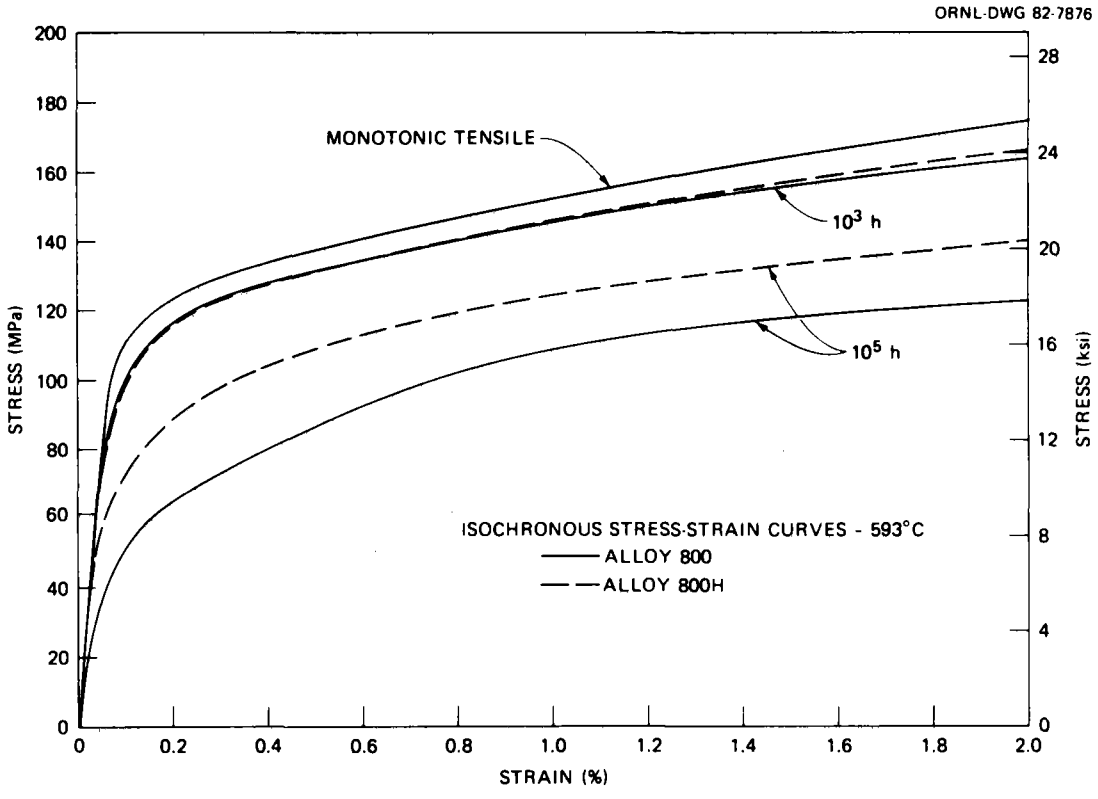

Fig. 19. Comparison of predicted isochronous stress-strain curves of mill-annealed alloy 800 and solution-annealed alloy 800H at 593°C.

SUMMARY

Available creep and creep-rupture data for the mill-annealed grade of the high-nickel austenitic alloy 800 were analyzed. Data were obtained

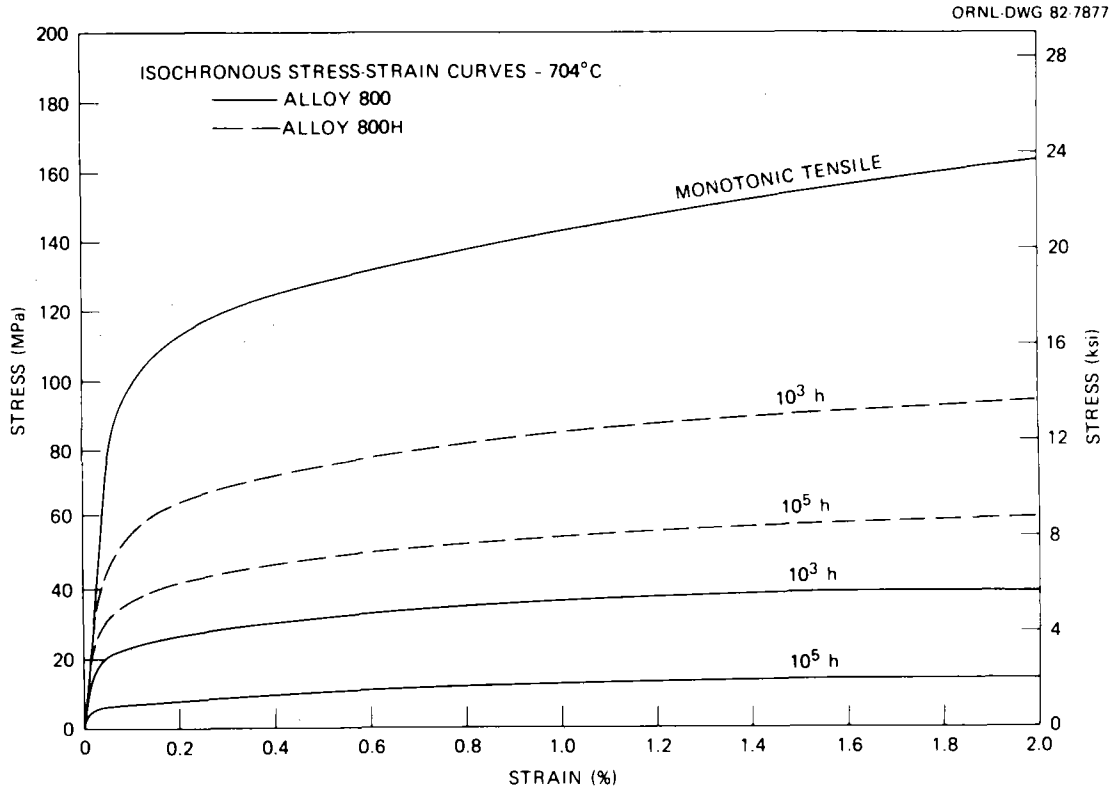

Fig. 20. Comparison of predicted isochronous stress-strain curves of mill-annealed alloy 800 and solution-annealed alloy 800H at 704°C.

from tests conducted over the temperature range from 450 to 760°C, with rupture lives extending from 10 h to about 19,000 h. The results yield analytical descriptions of the following properties: rupture life, minimum creep rate, time to the onset of tertiary creep, and creep strain-time behavior. The results are in a form that can be used directly in design calculations. However, the available data were limited, and all results of this report should be considered preliminary, especially in the case of the strain-time analysis.

ACKNOWLEDGMENTS

The author would like to thank J. P. Hammond and K. C. Liu for reviewing, Sigfred Peterson for editing, and Denise Sammons for preparing the final manuscript for this report.

REFERENCES

1. C. E. Sessions et al., *Review of the Behavior of Alloy 800 for Use in LMFBR Steam Generators,* WNET-115-R1, ORNL/SUB-4308/1, February 1976.

2. J. M. Martin, "Incoloy Alloy 800 Data for Use in Design of Gas Cooled and Liquid Metal Fast Reactors," presented at INCO/ORNL/RRD/WR&D/WTD Meeting on Development of an Advanced Material for Sodium Heated Steam Generators, Jan. 14, 1975.

3. C. E. Sessions and P. J. McGeehan, "ASME B&PV Code Recommendations of Design Stresses for Use of Annealed Alloy 800 in Elevated Temperature Nuclear Vessels," pp. 89–193 in *Status of Incoloy Alloy 800 Development for Breeder Reactor Steam Generators,* ORNL/SUB-4308/3, December 1978.

4. M. K. Booker and B.L.P. Booker, "New Methods for Analysis of Materials Strength Data for the ASME Boiler and Pressure Vessel Code," pp. 31–64 in *Use of Computers in Managing Material Property Data,* MPC-14, American Society of Mechanical Engineers, New York, 1980.

5. M. K. Booker, *Time-Dependent Allowable Stresses for ASME Code Case N-47 — A Second Look,* ORNL-5837, February 1982.

6. F. Garofalo et al., "Creep and Creep-Rupture Relationships in an Austenitic Stainless Steel," *Trans. Met. Soc. AIME* **221**, 310–19 (1960).

7. W. E. Leyda and J. P. Rowe, *A Study of Time for Departure from Secondary Creep for Eighteen Steels,* ASM Technical Report P9–6.1, American Society for Metals, Metals Park, Ohio, 1969.

8. M. K. Booker and V. K. Sikka, "A Study of Tertiary Creep Instability in Several Elevated-Temperature Structural Materials," pp. 325–43 in *Ductility and Toughness Considerations in Elevated Temperature Service,* MPC-8, American Society of Mechanical Engineers, New York, 1978.

9. D. L. Harrod, P. J. Langford, and D. M. Moon, "Relation of Physical Metallurgy to Mechanical Creep Behavior of Alloy 800," pp. 195–269 in *Status of Incoloy Alloy 800 Development for Breeder Reactor Steam Generators,* ORNL/SUB-4308/3, December 1978.

10. M. K. Booker, "An Analytical Representation of the Creep and Creep-Rupture Behavior of Alloy 800H," pp. 1–28 in *Characterization of Materials for Service at Elevated Temperatures*, MPC-7, American Society of Mechanical Engineers, New York, 1978.

11. L. D. Blackburn, "Isochronous Stress-Strain Curves for Austenitic Stainless Steels," pp. 15–48 in *The Generation of Isochronous Stress-Strain Curves*, American Society of Mechanical Engineers, New York, 1972.

12. M. K. Booker, "Analytical Description of the Effects of Melting Practice and Heat Treatment on the Creep Properties of 2 1/4 Cr-1 Mo Steel," pp. 323–43 in *Effects of Melting and Processing Variables on the Mechanical Properties of Steel*, MPC-6, American Society of Mechanical Engineers, New York, 1977.

13. F. V. Ellis, "Time-Temperature Parameter Based Incremental Creep Law for Finite Element Stress Analysis," pp. 29–50 in *Characterization of Materials for Service at Elevated Temperatures*, MPC-7, American Society of Mechanical Engineers, New York, 1978.

14. M. K. Booker, *Evaluation of Creep and Relaxation Data for Hastelloy Alloy X Sheet*, ORNL-5479, February 1979.

15. S. A. Sterling, *A Temperature-Dependent Power Law for Monotonic Creep*, GA-A13027 (Revised), General Atomic Co., San Diego, June 1974 (Revised March 1976).

16. A. B. Smith, "Revised Incoloy 800H Isochronous Stress-Strain Curves for Code Case 1592," unpublished document, General Atomic Company, San Diego, 1978.

Appendix

LOT-CENTERED REGRESSION ANALYSIS

Tensile Data

Yield and tensile strength are often expressed as simple polynomial functions of temperature:

$$\hat{S} = \sum_{i=0}^{N} b_i T^i \ , \tag{A1}$$

where

$\hat{S}$ = the predicted yield or tensile strength,

T = temperature, and

b_i = constants whose values are estimated by regression or other techniques.

In essence, the ratio technique involves an implicit assumption that different heats display parallel curves of log strength versus temperature. As a first step toward implementing this assumption in a direct data fit, Eq. (A1) can be rewritten as

$$\widehat{\log S} = \sum_{i=0}^{N} b'_i T^i \ . \tag{A2}$$

This equation is not equivalent to Eq. (A1) but would be expected to describe the data equally well.

Next, one employs a technique of centering the data for each lot, as has been reported for creep data by Sjodahl.[1] The equation thus becomes

$$\widehat{\log S_{hj}} - \overline{\log S_h} = \sum_{i=1}^{N} b'_i \left(T_{hj}^i - \overline{T_h^i} \right) \ , \tag{A3}$$

where the barred symbols represent average values of each variable for each lot. The index i again refers to the power of temperature, j refers to the particular test, and h refers to the particular lot. Equation (A3) can be arranged as

$$\widehat{\log S_{hj}} = \overline{\log S_h} + \sum_{i=1}^{N} b_i T_{hj}^i - \sum_{i=1}^{N} b_i \overline{T_h^i} , \tag{A4}$$

or as

$$\widehat{\log S_{hj}} = \left(\overline{\log S_h} - \sum_{i=1}^{N} b_i \overline{T_h^i}\right) + \sum_{i=1}^{N} b_i T_{hj}^i . \tag{A5}$$

Note that the quantity in parentheses is a constant (C_h) for a given lot. The other term on the right side of the equation is a function of temperature but not of lot. Thus, a fit of Eq. (A3) to the available data will yield for the different lots predictions that are parallel in log S versus T but have different intercept values. These intercept values are determined by a regression fit to all data, not merely by the room-temperature strength as in the ratio technique. In fact, lots for which no room-temperature data at all are available can be included in the lot-centered analysis. Such lots would, of course, have to be excluded from the ratio analysis. Note that since each lot has its own intercept, no explicit intercept term is required in the model in Eq. (A3).

If the assumption of log S versus T parallelism is not met, plots of strength ratio against temperature emphasize effects that cause the lack of parallelism. Likewise, residual plots of $(\log S - \widehat{\log S})$ against T from the above regression technique will point up such effects ($\log S$ is the log observed strength, $\widehat{\log S}$ is the log predicted strength). The regression technique can be used to determine a statistically defined average or minimum curve (see below), or these predictions can be keyed to

room-temperature values as in the ratio technique. Thus, the technique presented here includes all the advantages of the ratio technique but avoids its major disadvantages. However, this technique is suited only to computer analysis — not to manual analysis.

Creep Data

First assume that the logarithm of rupture life (log t_r)* has been chosen as the dependent variable for the analysis. Label log t_r as Y. Now assume that Y can be expressed as a linear function (in the regression sense) of terms involving stress (σ) and temperature (T). Label these terms as X_i. In general form we thus have

$$\hat{Y}_K = \sum_{i=0}^{N} a_i X_{iK} \ , \tag{A6}$$

where the a_i are constants estimated by regression and $\hat{Y}_K$ is the predicted value of log rupture life at the Kth level of the independent or predictor variables, X_{iK}. Note that X_0 is always unity and that a_0 is a constant intercept term.

As the next step, each variable (Y and all X) is "lot centered," and the equation becomes

$$\hat{Y}_{Kh} - \bar{Y}_h = \sum_{i=1}^{N} a_i'(X_{iKh} - \bar{X}_{ih}) \ , \tag{A7}$$

where the barred variables represent average values for a given lot and h represents the index of the lot involved. The prediction of log rupture life itself will then be given by

---

*The debate that has sometimes arisen over this choice is not central to the results obtained and will not be discussed here. The authors frankly do not feel that there is any legitimate question over the choice of dependent variable in this context.

$$\hat{Y}_{Kh} = \bar{Y}_h - \sum_{i=1}^{N} a_i' \bar{X}_{ih} + \sum_{i=1}^{N} a_i' X_{iKh} \cdot \qquad \text{(A8)}$$

The quantity $\hat{Y}_h - \sum_{i=1}^{N} a_i' \bar{X}_{ih}$ is a constant for a given heat and replaces the intercept term a_0 in the uncentered analysis. Thus, each lot will have a different intercept term, but all other coefficients a_i' will be common to all lots. (There is no separate a_0' term, because it would be superfluous.)

Lot centering the data involves no complicated mathematics and can be done by anyone who can add, subtract, and divide. However, for large data sets these simple operations can become quite tedious, and the centering is best done by computer. Implications of lot centering are also straightforward, although a first glance at Eq. (A8) can leave one lost in a maze of variables and subscripts.

As pointed out above, different lots are treated as having different intercept values, but all other equation constants are lot-independent. Thus, all lots vary similarly with the independent variable, but any two lots will always be separated by a constant increment in log t_r space. This assumption of parallelism may or may not be a good one in any given case.

If any lot is represented by a single datum, all lot-centered variables will be zero, and that lot will not contribute to establishment of stress and temperature dependence, although it will contribute to the calculation of average and minimum values as described below. If all data for a given lot occur at a single temperature, all pure temperature variables will be zero, and that lot will not contribute to the estimation of temperature dependence. Thus, lot-to-lot variation is addressed directly and vulnerability of the method to poorly distributed data is minimized.

Use of lot-centered models to predict average and minimum behavior is described in detail below. Suffice it to say here that the method certainly presents an estimate of the average far more reliable than that obtained from fitting the entire data base as a single population without regard to lot-to-lot variations. In its ability to separate the within-lot and between-lot variances, the method also offers superior possibilities for the estimation of minima.

The particular model form to use can be selected exactly as previously described by Booker.[2] Details of the model selection procedure will not be repeated here except to reemphasize the power and flexibility of the techniques involved. Literally tens of thousands of potential models can be explored and then reduced to a handful and finally to one with a minimum of tedium for the analyst. Some judgment is still involved, but that is considered more asset than liability. Any method relying strictly on computerized calculations without the opportunity for appropriate human intervention is dangerous at best.

The analyst makes several decisions along the way, but all actual computations are performed by machine. The final result is a single equation with perhaps three or four regression constants.

Calculation of Average and Minimum Strength by Regression on Lot-Centered Data

As described in the text, fitting a multilot set of creep-rupture data by use of lot-centered regression can yield results that accurately portray the stress and temperature dependences of the material under consideration. Predictions also include different intercept values to yield different strength levels for different lots or heats of material for which data are available. This section illustrates how an average strength level can also be predicted by the analysis. Finally, aspects of the method that lend themselves to accurate determination of minimum values are discussed, although detailed methods of defining minima are beyond the scope of this investigation. Results are discussed within the framework of rupture data because the models are more general. However, all discussions herein are equally applicable to tensile or any other data treated by this method.

First, return to Eq. (A7),

$$\hat{Y}_{Kh} - \overline{Y}_h = \sum_{i=1}^{N} a_i'(X_{iKh} - \overline{X}_{ih}) \quad . \tag{A7}$$

Here the barred variables represent simple arithmetic average values for a given lot of index h. The index i refers to the term in the model and K to

the particular datum within lot h. Equation (A7) is fit to the data as written, with $Y_{Kh} - \bar{Y}_h$ as the dependent variable, where Y_{Kh} is the experimental value of log t_r. However, because $\bar{Y}_h$ is a known constant for a given lot, all the error in prediction is in the estimation of $\hat{Y}_{Kh}$. Thus, when Eq. (A7) is fit to data by least squares and the a_i' are determined, the total "error" in fitting the model can be described by a residual sum of squares RSS, given by

$$\text{RSS} = \sum_{h=1}^{H} \sum_{K=1}^{M} (\hat{Y}_{Kh} - Y_{Kh})^2 \ . \tag{A9}$$

If there are n data total, RSS has a number of degrees of freedom df, given by

$$df = n - N - H \ , \tag{A10}$$

where N is the number of terms in the model and H is the number of lots (and thus the number of lot averages involved in the fitting).

By separating different lots through their different lot constants, this method attempts to describe only within-lot variations in behavior. No between-lot differences have been modeled at this point. Thus, the variance defined by the fit is an estimate of the pooled within-lot Variance V_w,

$$V_w = \text{RSS}/df \ . \tag{A11}$$

Equation (A7) can now be transformed to Eq. (A8),

$$\hat{Y}_{Kh} = \bar{Y}_h - \sum_{i=1}^{N} a_i' \bar{X}_{ih} + \sum_{i=1}^{N} a_i' X_{iKh} \tag{A8}$$

or

$$\hat{Y}_{Kh} = C_h + \sum_{i=1}^{N} a_i' X_{ikH} \ , \tag{A12}$$

where the differences in behavior of different lots are now explicitly defined in terms of the lot constants C_h, where

$$C_h = \overline{Y}_h - \sum_{i=1}^{N} a_i' \overline{X}_{ih} \ . \tag{A13}$$

Because C_h is a single constant for a given lot, estimation of average behavior consists only of estimating the average lot constant $\overline{C}_h$. Two methods immediately suggest themselves. First, one might choose to define $\overline{C}_h$ as the arithmetic mean of the C_h. Indeed, if the between-lot variability is much larger than the within-lot variability, such an approach would be justified. However, if the amount of within-lot variability is significant, the estimates of C_h will contain some error. Lots with more data will have a better estimate of C_h than will lots with fewer data. Thus, not all lots should be weighted equally.

Perhaps each lot should be weighted according to the number of data available for that lot. This approach is correct only if the within-lot variability is much larger than the between-lot variability. If not, this procedure (which weights each *test* equally) is not valid, because no one lot is necessarily more "important" in the collection of lots available, even if it is represented by more data.

A possible solution comes from the work of Mandel and Paule,[3] who studied variations in behavior caused by measurements of chemical variables at different laboratories. After Sjodahl,[1] we extrapolate Mandel's lab-to-lab variation results to our lot-to-lot variation data. Following this approach, we find that the C_h for each lot should be given a weight w_h of

$$w_h = k_h/(k_h\lambda + 1) \ , \tag{A14}$$

where k_h is the number of data for lot h and λ is V_B/V_w, where V_B is the between-lot variance for the lots involved. Knowing the appropriate weights, $\bar{C}_h$ can be calculated by

$$\bar{C}_h = \sum_{h=1}^{H} C_h w_h / \sum_{h=1}^{H} w_h \ . \tag{A15}$$

Unfortunately, the w_h cannot be estimated at this point because V_B and thus λ are unknown. As a result, we have one equation in two unknowns, and a solution can be obtained only by iterative techniques. However, such techniques are easily implemented by computer.

Mandel and Paule[3] present an iterative technique, which does indeed result in a solution for both $\bar{C}_h$ and V_B. Our experience is that results are obtained typically after only three or four iterations. Sjodahl[1] has reported similar quick convergence to a solution. The result is probably the most fairly weighted estimate of average behavior obtainable by any technique proposed to this point.

Note also that by the direct separation of the variability into its two components V_B and V_w, this method also yields better estimates of error than could be obtained by estimates of error that are a mixture of within-lot and between-lot variability, with no clear meaning. Because variance estimation is central to the estimation of any statistical limit, regression on lot-centered data thus also opens the way for superior techniques to estimate these limits.

References

1. L. H. Sjodahl, "A Comprehensive Method of Rupture Data Analysis with Simplified Models," pp. 501–15 in *Characterization of Materials for Service at Elevated Temperatures*, MPC-7, American Society of Mechanical Engineers, New York, 1978.

2. M. K. Booker, "Use of Generalized Regression Models for the Analysis of Stress-Rupture Data," pp. 459–99 in *Characterization of Materials for Service at Elevated Temperatures*, MPC-7, American Society of Mechanical Engineers, New York, 1978.

3. J. Mandel and R. C. Paule, "Interlaboratory Evaluation of a Material with Unequal Numbers of Replicates," *Anal. Chem.* 42: 1194–97 (1970); corrected in *Anal. Chem.* 43: 1287 (1971).

INTERNAL DISTRIBUTION

1–2. Central Research Library
3. Document Reference Section
4–5. Laboratory Records Department
6. Laboratory Records, ORNL RC
7. ORNL Patent Section
8–12. M. K. Booker
13. C. R. Brinkman
14. J. A. Clinard
15. J. M. Corum
16–18. F. R. Cox
19. J. R. DiStefano
20. J. P. Hammond
21. R. L. Huddleston
22. H. E. McCoy
23. J. C. Ogle
24. A. R. Olsen
25. G. F. Petersen
26. C. E. Pugh
27. G. M. Slaughter
28. R. W. Swindeman
29. C. L. White
30. M. H. Yoo
31. R. J. Charles (Conslutant)
32. Alan Lawley (Consultant)
33. T. B. Massalski (Consultant)
34. R. H. Redwine (Consultant)
35. J. C. Williams (Consultant)
36. K. M. Zwilsky (Consultant)

EXTERNAL DISTRIBUTION

37. Argonne National Laboratory, Materials Science Division, 9700 South Cass Ave., Argonne, IL 60439

    S. Majumdar

38. Arizona Public Service Co., P.O. Box 21666, Phoenix, AZ 85036

    E. Weber

39. Babcock & Wilcox, 20 S. Van Buren Ave., Barberton, OH 44203

    G. Grant

40. Bechtel Corporation, P.O. Box 3965, San Francisco, CA 94119

    E. Lam

41. Black & Veatch Consulting Engineers, P.O. Box 8405, Kansas City, Mo 64114

    J. C. Grosskreutz

42. Combustion Engineering, Inc., 1000 Prospect Hill Rd., Windsor, CT 06095

    C. R. Buzzoto

43. Electric Power Research Institute, P.O. Box 10412, 3412 Hillview Ave., Palo Alto, CA 94303

E. DeMeo

44–46. Foster Wheeler Development Corp., 12 Peachtree Hill Rd., Livingston, NJ 07039

R. J. Zoschak
I. Berman
T. V. Narayanan

47. General Atomic Company, P.O. Box 81608, San Diego, CA 92138

J. L. Kaae

48. Martin Marietta Corp., P.O. Box 179, M/S L0450, Denver, CO 80201

T. R. Tracey

49–50. McDonnell Douglas Astronautics Company, 5301 Bolsa Ave., Huntington Beach, CA 92647

R. L. Gervais
G. Coleman

51. Pacific Gas & Electric, Dept. of Engineering Research, 3400 Crow Canyon Rd., San Ramon, CA 94583

H. E. Seielstad

52. Rockwell International, Energy Systems Group, 8900 De Soto Ave., Canoga Park, Ca 91304

T. H. Springer

53. Rockwell International, Rocketdyne Division, 6633 Canoga Ave., Canoga, Park, CA 91304

R. Surette

54–55. Solar Energy Research Institute, 1617 Cole Blvd., Golden, CO 80401

B. L. Butler
B. P. Gupta

56. Southern California Edison, P.O. Box 800, Rosemead, CA 92807

J. N. Reeves

57. Stearns-Roger Engineering Corp., P.O. Box 5888, Denver, CO 80217

W. R. Lang

58–60. Sandia National Laboratories, P.O. Box 5800, Albuquerque, NM 87185

M. J. Davis, Dept. 1830
W. B. Jones, Div. 1832
C. H. Karnes, Div. 1835

61–69. Sandia National Laboratories, P.O. Box 969, Livermore, CA 94550

W. A. Kawahara, Div. 8123
R. W. Rohde, Dept. 8310
D. A. Hughes, Div. 8316
T. C. Lowe, Div. 8316
J. C. Swearingen, Div. 8316
J. B. Wright, 8450
A. C. Skinrood, 8452
W. G. Wilson, 8453
D. B. Dawson, 8454

70. Westinghouse Electric Corp., Advanced Energy Systems Division, P.O. Box 10864, Pittsburgh, PA 15236

D. S. Griffin

71–74. U.S. Department of Energy, Division of Solar Thermal Technology, Forrestal Building, Room 5H021I, Code CE-314, 1000 Independence Ave., S. W., Washington, DC 20585

G. W. Braun
K. T. Cherian
C. B. McFarland
M. R. Scheve

75. U. S. Department of Energy, San Francisco Operations Office, 1333 Broadway, Oakland, CA 94612

R. W. Hughey

76. DOE, OAK RIDGE OPERATIONS OFFICE, P.O. Box E, Oak Ridge, TN 37830

Office of Assistant Manager for Energy Research and Development

77-103. DOE, TECHNICAL INFORMATION CENTER, Office of Information Services, P.O. Box 62, Oak Ridge, TN 37830

For distribution as shown in TID-4500 Distribution Category,
UC-79h (Structural Materials and Design Engineering)
UC-79k (Components)
UC-79r (Structural and Component Materials Development)